

# Photoinduced Charge Separation after Excited Energy Transfer in Snowflake-Shaped Zn–Porphyrin Dendrimer with Anthraquinone Terminals: Enhancement of the Electron-Transfer Rates by “Dendrimer Effect”

Masatoshi Kozaki,<sup>\*1</sup> Kogen Akita,<sup>1</sup> Keiji Okada,<sup>\*1</sup> D.-M. Shafiqul Islam,<sup>2</sup> and Osamu Ito<sup>\*2</sup>

<sup>1</sup>Graduate School of Science, Osaka City University, 3-3-138 Sugimoto, Sumiyoshi-ku, Osaka 558-8585

<sup>2</sup>Institute of Multidisciplinary Research for Advanced Materials, Tohoku University, Katahira, Sendai 980-8577

Received February 19, 2010; E-mail: kozaki@sci.osaka-cu.ac.jp

Photoinduced electron transfer (ET) and energy transfer (EnT) of a snowflake-shaped Zn–porphyrin dendrimer with anthraquinone terminals (dendrimer-1), which has four rigid ethynylene–phenylene conjugated chains covered by soft benzyl ether (BE) branches, is investigated by means of steady-state and time-resolved fluorescence measurements. Dendrimer-2 without anthraquinone terminals undergoes a nearly quantitative EnT from the excited singlet states of BE branches to the Zn–porphyrin core, where the conjugated chain plays an important role as a mediator of EnT within this antenna type dendrimer (the dendrimer effect on EnT). A comparison of the rates of charge separation via the singlet excited state of Zn–porphyrin to the anthraquinone terminals through oligo(ethynylene–phenylene)s in a series of model compounds reveals considerable acceleration of the rate constants by the dendrimer architecture (the dendrimer effect on ET). This acceleration is attributed to hydrophobic interactions between the flexible BE chains within dendrimer-1, resulting in a significant conformational change into coplanar forms between the Zn–porphyrin plane and the ethynylene–phenylene–anthraquinone plane.

Dendritic structures are quite attractive for the construction of a well-organized assembly with a large number of functional groups.<sup>1</sup> One of the most attractive applications of dendritic architectures is to construct artificial photosynthetic molecular devices containing chromophores that are arranged for light harvest and charge separation (CS). Many artificial light harvesting systems have thus far been constructed with the incorporation of a variety of chromophores, such as porphyrins,<sup>2</sup> oligo(ethynylene–phenylene)s,<sup>3</sup> and naphthalimides<sup>4</sup> into the dendrimer architectures.<sup>5,6</sup> Efficient light harvesting processes from dendritic branches into a core have been observed, although the efficiency of these process is generally dependent on the generation size in the dendrimers.<sup>3a</sup> Moreover, a nearly 100% energy transfer (EnT) can be realized by introduction of the energy gradients into the dendritic chains.<sup>3</sup>

However, a difficulty in dendrimer architecture is often encountered when one uses the harvested light energy as a chemical potential through electron-transfer processes. In fact, there have been only a few reports on dendritic systems that function as both light harvesting and successive CS systems,<sup>6</sup> even as CS systems alone have been incorporated in dendrimer frameworks.<sup>4b,7</sup> Natural photosynthetic systems employ the strategy of integrated molecular systems, in which the reaction center for the CS is precisely positioned inside the multiple light harvesting antennas.<sup>8</sup> A simpler approach may be possible through the incorporation of a new channel of electron transfer (ET) besides the dendritic branches into a dendrimer framework. This new channel (a favorably  $\pi$ -conjugated system)<sup>9</sup> must combine the energy-harvested core (the electron donor,

for instance) with peripheral new electron acceptors. In such a system, excitation of the energy donors embedded in dendritic branches causes an energy migration to the core (energy acceptor and electron donor) through-bonds and through-space, followed by the fast ET from the excited core to the peripheral electron acceptors through the newly added channels.

We have recently reported a convergent synthetic methodology for snowflake-shaped dendrimers in which conjugated chains, oligo(ethynylene–phenylene)s (abbreviated as EtPh), were incorporated inside the benzyl ether (BE) dendritic branches.<sup>10</sup> The dendrimer with a 1,3,5-trisubstituted benzene core showed highly efficient BE fluorescence quenching in steady-state measurements, which was reasonably interpreted by EnT from the <sup>1</sup>BE\* to the EtPh-conjugated chains. The convergent method was successfully applied to the construction of the Zn–porphyrin dendrimer with anthraquinone (AQ) units at the terminal of the conjugated chains. As a preliminary finding, we reported the quenching of the Zn–porphyrin fluorescence by the AQ units.<sup>11</sup> The strategy of this dendrimer design is quite different from that of previous approaches. The advantages of this type of dendrimer are as follows: 1) Coupling of the dendritic antenna provides a versatile synthetic approach that is applicable to various donor–bridge–acceptor systems, 2) the distance between the electron donor and electron acceptors is fixed by the rigid conjugated chain, allowing a clear argument for mechanistic points of view, and 3) because of the symmetric structure of the dendrimer, the efficiency of the photoinduced ET process can be directly compared to the corresponding dendron and/or their building

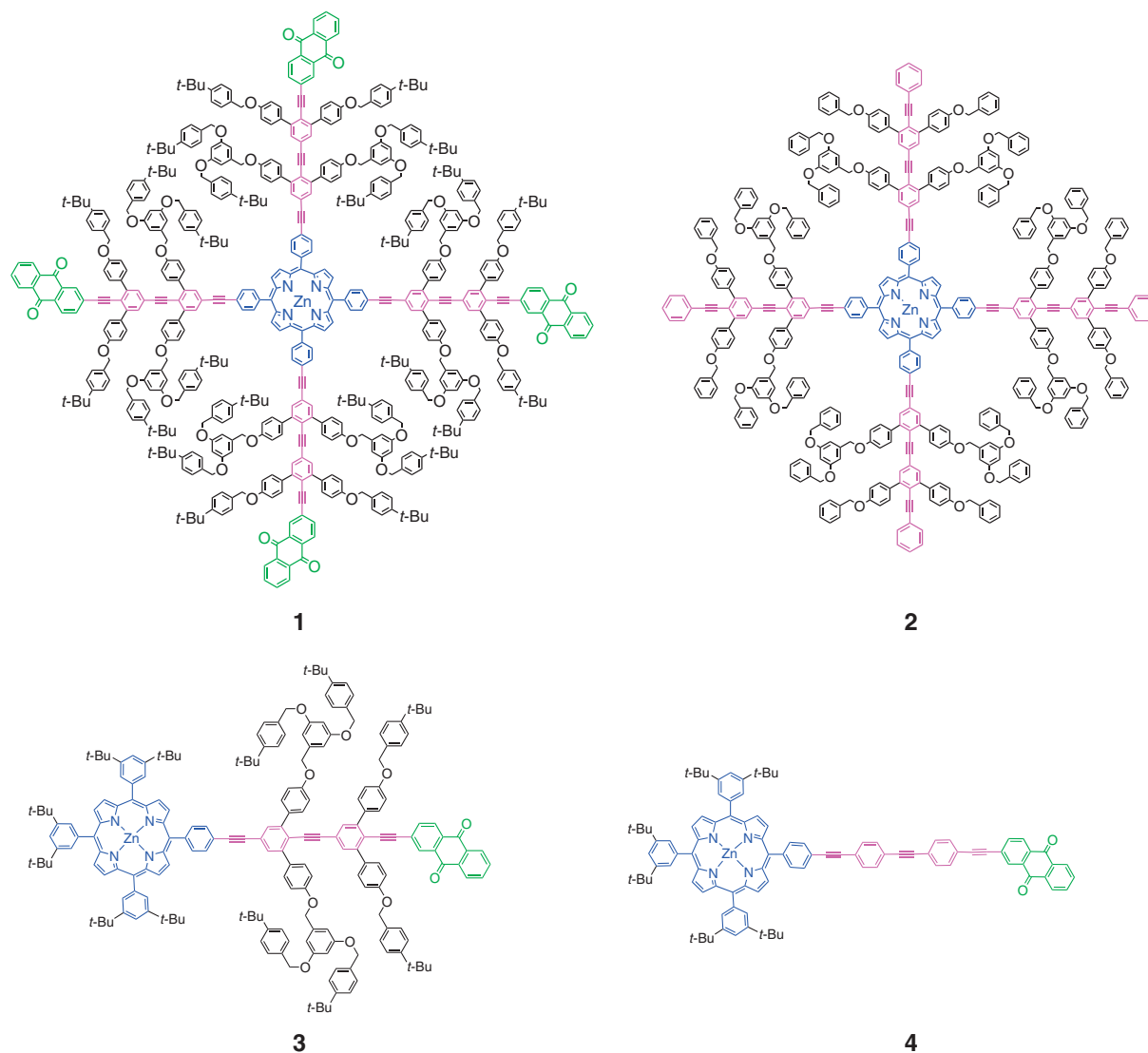


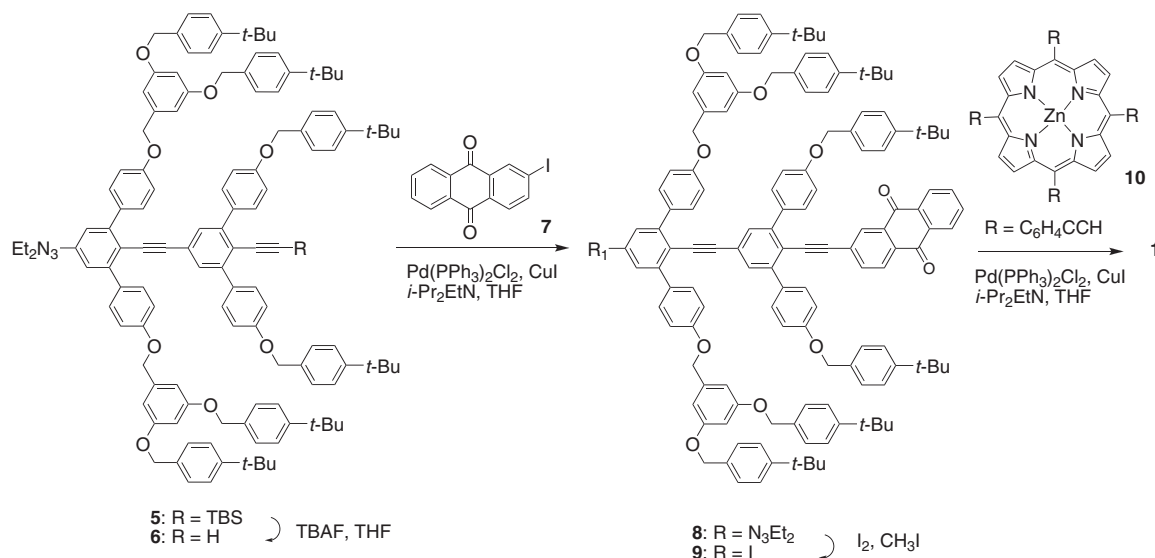
**Chart 1.** Chemical structures of snowflake-shaped Zn-porphyrin dendrimers and reference compounds.

blocks, providing important information on the relationship between the structure and efficiency of the ET. In addition, the snowflake-shaped dendrimers are expected to serve as modular building blocks<sup>10c</sup> for an integrated molecular system of biomimetic photosynthesis. In order to design such integrated multifunctional dendrimer systems, it is essential to establish the mechanism by which the ET efficiency is influenced by the dendrimer architecture. In this paper, we report upon the photophysical properties of novel snowflake-shaped Zn-porphyrin dendrimers with the AQ and phenyl terminals, dendrimer-1 and dendrimer-2, respectively, and related compounds 3 and 4 (Chart 1). Significant enhancement of EnT efficiency in dendrimer-2 (the dendrimer effect on EnT) and ET efficiency in dendrimer-1 (the dendrimer effect on ET) was observed in time-resolved fluorescence measurements. The origin of these dendrimer effects is discussed in detail.

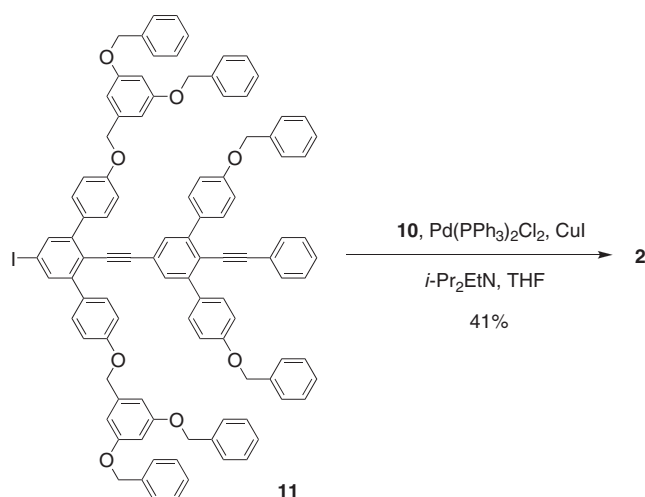
### Results and Discussion

**Synthesis.** First, dendron 5 was prepared by the previously reported convergent method<sup>10a,11</sup> which employs Suzuki-

Miyaura coupling,<sup>12</sup> iodation,<sup>13</sup> and Sonogashira coupling reactions.<sup>14</sup> The anthraquinon-2-yl terminals were attached to the dendron 5 by removal of the TBS groups in dendron 5, followed by the Sonogashira coupling reaction with 2-iodoanthraquinone (7)<sup>15</sup> (Scheme 1). Dendron 8 was heated with iodine in iodomethane to give dendron 9. The Sonogashira coupling reaction of Zn-porphyrin core 10<sup>16</sup> with dendron 9 yielded the desired dendrimer-1 in the form of a purple powder. Dendrimer-2 was also successfully prepared by the Sonogashira coupling reaction of the phenyl-terminated dendron 11 and porphyrin core 10 (Scheme 2). The reference compounds 3 and 4 were obtained by employing a similar method (Schemes 3 and 4). These compounds were soluble in various organic solvents such as chloroform, dichloromethane, THF, and toluene and were unambiguously characterized by means of NMR, elemental analysis, and MALDI-TOF mass spectroscopy. Interestingly, the <sup>1</sup>H NMR spectra of dendrimer-1 and dendrimer-2 showed broad signals at room temperature. Sharp and well-resolved signals were obtained at higher temperatures (at 135 °C for dendrimer-1 and 85 °C for dendri-



Scheme 1. Synthesis of dendrimer-1.



Scheme 2. Synthesis of dendrimer-2.

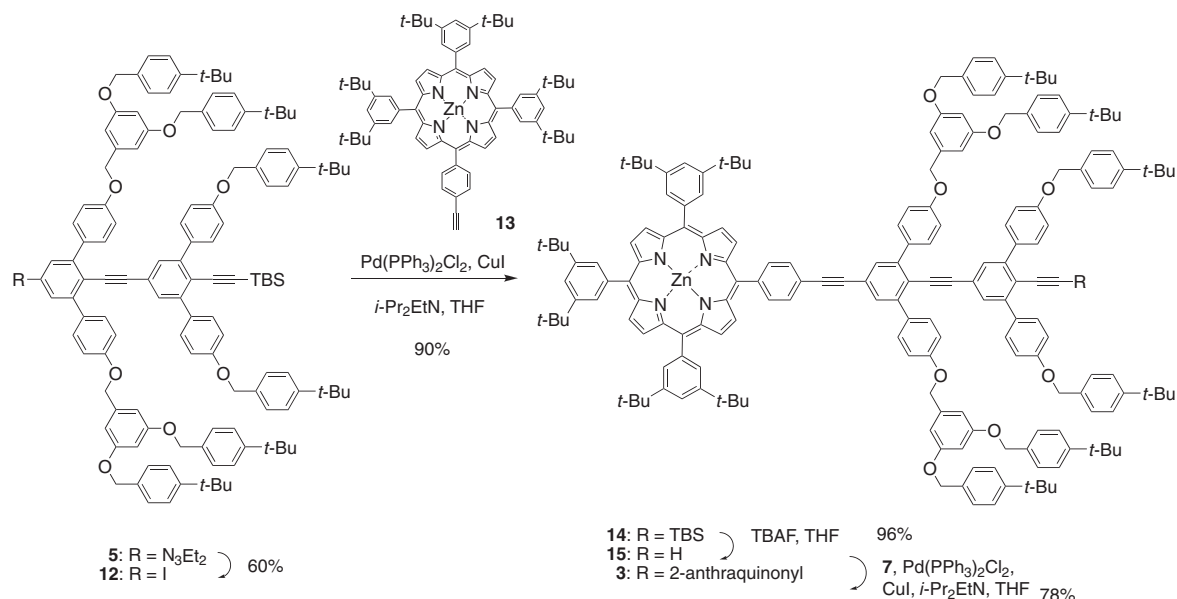
mer-2) in tetrachloroethane-*d*<sub>2</sub> (see Supporting Information (SI)). Similar behavior was reported for the snowflake-shaped dendrimer with a 1,3,5-substituted benzene core.<sup>10a</sup> On the contrary, normal Fréchet type (BE type) porphyrin dendrimers have been reported to exhibit sharp NMR signals at room temperature.<sup>17</sup> These results suggest that the equilibria that are present between various conformers are probably due to slow rotation around the ethynylene bonds in EtPh units that are covered by bulky flexible BE chains in dendrimer-1 and dendrimer-2.

**Electronic Absorption Spectra.** Figure 1 shows the UV–vis absorption spectra of dendrimers-1 and -2, dendron-3, and dyad-4 in THF. Dendrimer-1 shows the characteristic bands of a Zn–porphyrin unit (Soret band:  $\lambda_{\text{max}} = 431$  nm, Q-bands:  $\lambda_{\text{max}} = 565, 609$  nm, Table 1) along with absorption bands due to the branched BE chains ( $\lambda_{\text{max}} = 256$  nm) and the conjugated EtPh chains ( $\lambda_{\text{max}} = 377$  nm). The Soret absorption peaks of the Zn–porphyrin core of dendrimer-1 and dendrimer-2 (433 nm) exhibit slight bathochromic shifts in comparison

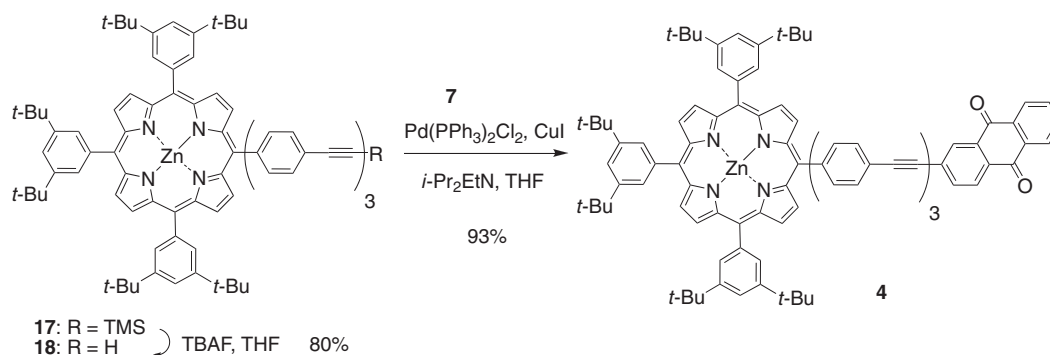
with Zn–tetraphenylporphyrin (Zn–TPP at 423 nm), suggesting that the covalent linkage of conjugated EtPh chains slightly expands the  $\pi$ -conjugation. Importantly, dendrimer-1 with AQ-terminals (<400 nm) exhibits Soret band that is considerably broader than those for dendrimer-2 and the reference compounds 3 (427 nm) and 4 (427 nm). The shape of the Soret band of dendrimer-1 was independent of the concentration in the range between  $2.5 \times 10^{-7}$  and  $2.5 \times 10^{-6}$  M. This result rules out the possibility of intermolecular aggregate formation.<sup>18</sup> Further, the sharp absorption of dendrimer-2 suggests that the broadening of dendrimer-1 is not related to structure factors possibly caused by deformation in the core porphyrin ring,<sup>19</sup> but rather, to the presence of the AQ groups. Interestingly, the Soret bandwidth of dendrimer-1 is strongly dependent on solvent polarity. Broader absorption was observed in more polar solvents (full width at half maximum (fwhm) = 30–37 nm in THF and 1,4-dioxane, fwhm = 43–44 nm in DMF and benzonitrile (See SI)), indicating that there is weak electronic communication between the Zn–porphyrin core and the AQ-units via the EtPh-bridges in the dendrimer-1 in the ground state accompanying the change of dipole moments.<sup>20</sup>

**Dendrimer Effect on Energy Transfer.** An energy diagram of the local excited states in dendrimer-2 is shown in Figure 2. The highest energy state belongs to the branched BE-chain. Although the absorption of each BE-branch is not high, 48 benzene rings moderately absorb the UV light to give <sup>1</sup>BE\*. The EnT can then proceed in the sequence of <sup>1</sup>BE\* → <sup>1</sup>EtPh\* → <sup>1</sup>Zn–porphyrin\*. Alternatively, a direct EnT from <sup>1</sup>BE\* to Zn–porphyrin is possible.

The absorption of conjugated EtPh-chains in dendrimer-2 observed around 370 nm sufficiently overlaps the emission of the BE-branch around 310 nm.<sup>2b</sup> In addition, the EtPh-chains in dendrimer-2 are expected to have emission around 440 nm,<sup>10a</sup> the value at which the Zn–porphyrin has its intense Soret absorption. These observations suggest that the conjugated EtPh-chain effectively mediates the excited singlet EnT from the BE-branches to the Zn–porphyrin core by the Förster mechanism. To evaluate the efficiency of the EnT from the



Scheme 3. Synthesis of dendron 3.



Scheme 4. Synthesis of dyad 4.

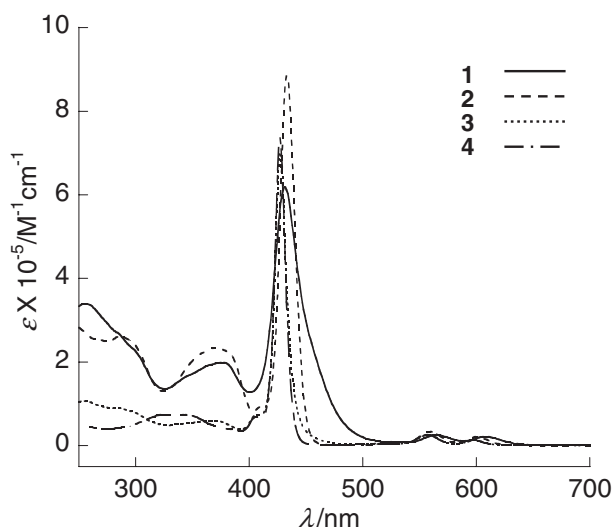


Figure 1. UV-vis absorption spectra of 1–4 in THF.

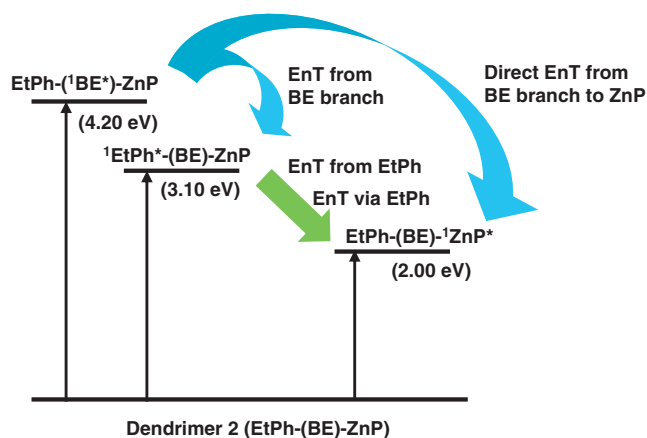
BE-branch to the Zn-porphyrin core via the EtPh-chain, the steady-state fluorescence spectra of dendrimer-2 were measured in THF by changing the excitation wavelength (Figure 3).

Table 1. Photophysical and Electrochemical Properties of 1–4

Compd	$\lambda_{\text{ABmax}}^{\text{a)}}$ /nm	Emission <sup>b)</sup>		$E_{\text{ox}}^{\text{c)}$	$E_{\text{red}}^{\text{c)}$
		$\lambda_{\text{EMmax}}^{\text{a)}}$ /nm			
1	256, 377, 431, 565, 609	625	— <sup>d)</sup>	— <sup>d)</sup>	−0.86
2	286, 372, 433, 560, 601	613, 658	— <sup>d)</sup>	— <sup>d)</sup>	—
3	255, 284, 370, 427, 558, 598	605, 656	0.74	−0.81	—
4	343, 427, 559, 598	606, 655	0.74	−0.76	—

a) In THF. b) In THF, excitation at Soret band. c) In 1,2-dichloroethane, V vs. SCE, scan rate 100 mV s<sup>−1</sup>, Pt disk was used as a working electrode. d) Not observed due to the slow electron-transfer rate between a redox center and the electrode.

Under excitation of the BE-branch at 286 nm, a value at which both the EtPh-conjugated chain and the Zn-porphyrin core have only weak absorption, an intense fluorescence of the Zn-porphyrin core appeared at 600–700 nm as shown in Figure 3a, suggesting efficient EnT from <sup>1</sup>BE\*<sup>−</sup> units to the Zn-porphyrin core. Both direct excitation of the Zn-porphyrin core and sensitized excitation of the BE-branch gave the same Zn-porphyrin fluorescence with an identical quantum efficiency ( $\Phi_{\text{F}}$ ) of 0.05. Furthermore, the excitation of the EtPh-units



**Figure 2.** Energy diagram for dendrimer-2 (EtPh-(BE)-ZnP) (EtPh: oligo(ethynylphenylene)s conjugated chain, and BE: oligo(benzyl ether) branch, and ZnP: Zn-porphyrin core, EnT: energy transfer).

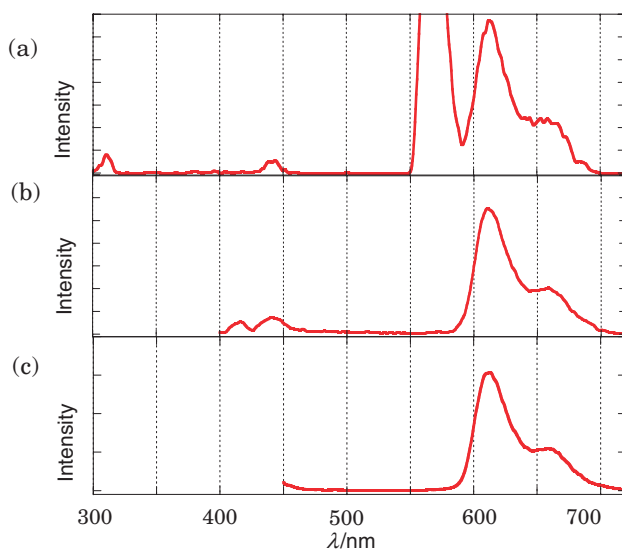


**Figure 3.** Steady-state fluorescence spectra of dendrimer-2 in THF. (a) 286-nm excitation (the intense peak at 572 nm is the scattered overtone of excitation light). (b) 372-nm excitation (a weak peak at 415 nm is due to the scattered excitation light). (c) 433-nm excitation.

(372 nm) also induced Zn-porphyrin fluorescence with an identical quantum yield ( $\Phi_F = 0.05$ ), as shown in Figure 3b. These results indicate that highly efficient (ca. 100%) intramolecular singlet EnT takes place both from the branched BE-chains and the conjugated EtPh-chain to the Zn-porphyrin core. Therefore, the overall fluorescence intensity from the Zn-porphyrin core under broad-band light excitation should be increased by the BE-excitation (286 nm) and EtPh-excitation (372 nm), in addition to the direct excitation of Zn-porphyrin (431, 565, and 609 nm for dendrimer-2).

Obviously, the dendrimer structure offers the great advantage of incorporating a large number of BE-branches and/or EtPh-chains; from their excited states, nearly quantitative EnT occurs, as is schematically illustrated in Figure 4. This

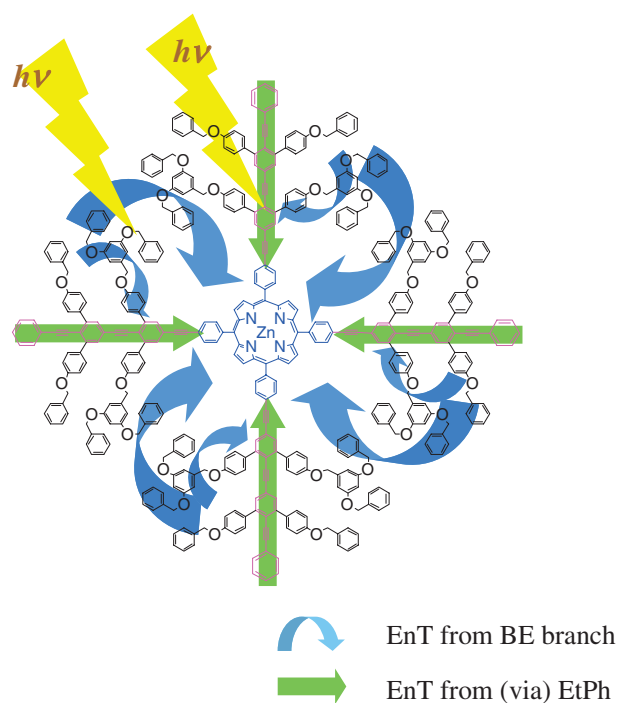


**Figure 4.** Schematic illustration of dendrimer effect on EnT in dendrimer-2 showing the enhancement of fluorescence of the Zn-porphyrin core by the excitation of dendrons (BE branches and EtPh chains).

molecular design is quite useful for obtaining an intense fluorescence from the core by utilizing absorptions due to a large number of energy donor chromophores through efficient EnT in dendrimer frameworks.<sup>4d,4e</sup>

It is interesting to compare the present results with those of closely related Zn-porphyrin dendrimer systems without conjugated chains. Jiang and Aida reported a dendrimer with similar BE-branches and a Zn-porphyrin core; the efficiency of EnT from the BE-chains to the core Zn-porphyrin (direct EnT in Figures 2 and 4) in a dendrimer of similar size was reported as 54%.<sup>2b</sup> Moreover, it has been well documented that there is a limit in the generation size for the EnT process in this type of dendrimer framework.<sup>3a</sup>

The high efficiency of EnT observed in dendrimer-2 strongly indicates that the EtPh-conjugated chain plays an important role as a mediator for the EnT from the branching BE-chains to the Zn-porphyrin core.<sup>4d,4e</sup> This mediator effect (the dendrimer effect on EnT) is very useful to the design of a larger antenna system.

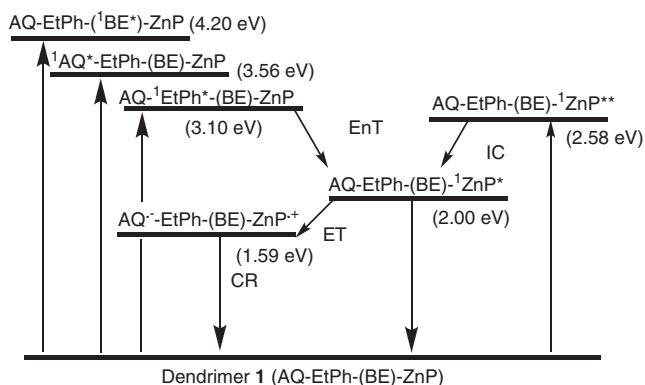
**Redox Potentials and Energy Diagram in Electron Transfer.** In the previous section, we have shown that efficient EnT can be realized by the combination of the BE chains and EtPh conjugate chains in dendrimer-2, a process which should be applicable to dendrimer-1 with the AQ-terminals. The accumulated excited energy in the porphyrin core can be utilized as a chemical potential by introducing the AQ-electron acceptors as terminals of the conjugate chains.

Cyclic voltammograms of 1-4 were measured in 1,2-dichloroethane ( $\epsilon = 10.36$ ) containing tetra-*n*-butylammonium perchloride as a supporting electrolyte using a Pt disk, Pt wire, and SCE as working, counter, and reference electrodes,

**Table 2.** Steady-State Fluorescence Quenching Efficiency and Free Energy Changes in Electron Transfer within Dendrimer-1

Solvent	$\epsilon$	Quenching efficiency/% <sup>a)</sup>	$\Delta G_{ET}/\text{eV}^{\text{b)}$
1,4-Dioxane	2.21	30 (38)	+0.36
THF	7.58	69 (73)	−0.41
Benzonitrile	25.7	90 (89)	−0.63
DMF	36.7	98 <sup>c)</sup> (93 <sup>c)</sup>	−0.66

a) Estimated from the fluorescence quantum yields. Values in parentheses were calculated using the weighted average charge separation rate constant  $(k_{CS})_w$  as  $(k_{CS})_w / ((k_{CS})_w + 0.63 \times 10^9)$ ; see Table 4. b) Obtained using the Rehn–Weller approximation<sup>7d,22</sup> ( $E_{ox}(\text{Por}) = 0.74$  V vs. SCE,  $E_{red}(\text{AQ}) = -0.81$  V vs. SCE,  $E_{0-0} = 2.00$  eV,  $R_{DA} = 29.0$  Å). Effective ionic radii of the donor and acceptor were assumed to be 5 Å.<sup>7d,22b</sup> c) Weighted average.

**Figure 5.** Energy diagram of dendrimer-1 (AQ–EtPh–(BE)–ZnP) in THF, where \* and \*\* denote the first and the second excited states, respectively.

respectively. Dendrimer-1 and dendrimer-2 showed significantly broad redox waves due to the slow ET rate between the encapsulated porphyrin core and the electrode.<sup>21</sup> On the other hand, dendron-3 and dyad-4 showed clear reversible redox waves at 0.74 V vs. SCE, which are attributed to the oxidation ( $E_{ox}$ ) of the Zn–porphyrin units (Table 1). The redox waves corresponding to the reduction ( $E_{red}$ ) of the AQ-terminals in 3 and 4 were observed at −0.81 and −0.76 V vs. SCE, respectively.<sup>15</sup> From these electrochemical data, the energy level ( $\Delta G_{RIP}$  in eV) of the radical ion pair Zn–porphyrin<sup>+</sup>/AQ<sup>−</sup> within dendrimer-1, as estimated by the Rehn–Weller approximation,<sup>7d,22</sup> is 1.59 eV above the ground state in THF ( $\epsilon = 7.58$ ), using the center-to-center ( $R_{DA}$ ) distance between the Zn–porphyrin core and AQ-terminal = 29.0 Å.<sup>23</sup> Thus, the ET from <sup>1</sup>Zn–porphyrin\* ( $E_{0-0} = 2.00$  eV) to the AQ-terminals within dendrimer-1 in THF is an exothermic process;  $\Delta G_{ET} = -0.41$  eV (Table 2). Figure 5 illustrates the energy levels of possible radical ion pairs and the local excited states in dendrimer-1 (AQ–EtPh–(BE)–ZnP) in THF.

#### Steady-State Fluorescence Quenching in Dendrimer-1.

The fluorescence from the Zn–porphyrin core (431-nm excitation) was effectively quenched by the AQ-moiety (in dendrimer-1, dendron-3, and dyad-4) in polar solvents (benzonitrile and DMF), whereas dendrimer-2 showed the strongest fluo-

rescence because of the absence of the AQ-unit. The quenching efficiency increased in the order of dyad-4 (89%) < dendron-3 (95%) < dendrimer-1 (98% quenching) in DMF. The quenching efficiency of dendrimer-1 was strongly solvent-dependent [30% quenching ( $\Phi_F = 0.04$ ) in 1,4-dioxane ( $\epsilon = 2.21$ ), 69% quenching ( $\Phi_F = 0.02$ ) in THF ( $\epsilon = 7.58$ ), 90% quenching ( $\Phi_F = 0.007$ ) in benzonitrile ( $\epsilon = 25.7$ ), 98% ( $\Phi_F = 0.001$ ) quenching in DMF ( $\epsilon = 36.7$ )], as summarized in Table 2.

The EnT from <sup>1</sup>Zn–porphyrin\* to the AQ-terminal cannot be considered an origin of Zn–porphyrin fluorescence quenching, because of a highly endothermic process. On the other hand, the ET from <sup>1</sup>Zn–porphyrin\* to the AQ-terminal can be an origin of Zn–porphyrin fluorescence quenching, because of an exothermic process in polar solvents. Table 2 shows the quenching efficiency and the free energy change in the electron transfer from <sup>1</sup>Zn–porphyrin\* to the AQ-terminal for dendrimer-1, which indicate that both the quenching efficiency and the free energy changes<sup>7d,22</sup> are strongly dependent on the solvent polarity; the ET-reaction is thermodynamically more favored in more polar solvents, supporting the idea that the electron transfer is the origin of Zn–porphyrin fluorescence quenching. A similar trend was observed for the encapsulated dendron-3 and the uncovered dyad-4, which exhibit a free energy change similar to that of dendrimer-1, although the quenching efficiencies are lower than those of dendrimer-1 in all the solvents. A lower degree of quenching was observed in 1,4-dioxane for dendron-3 and dyad-4 because of the positive free energy in 1,4-dioxane. The higher quenching efficiency of dendrimer-1 as compared to that of dendrons-3 and dyad-4 is probably not related to the free energy term, but rather, to the kind and number of dendrons. This will be discussed in more detail in the sections, “Modeling Study of dyad-4” and “Dendrimer Effect and Mechanism of Electron Transfer.”

#### Kinetic Study of Fluorescence Quenching in Dendrimer-1.

In order to obtain a deeper insight into the fluorescence quenching, we measured the time-profiles of the fluorescence intensity of the Zn–porphyrin core under picosecond laser light excitation at 410 nm using a streak-scope (Figure 6). The fastest decay was observed for dendrimer-1. Moderately fast decay was observed for dendron-3. The slowest fluorescence decay was observed for dyad-4 (Figure 6a). The fluorescence lifetime ( $\tau_F$ ) of dendrimer-2 was almost solvent-independent, which is consistent with no ET quenching. Therefore, dendrimer-2 can be used as a reference compound that provides a standard decay rate without ET;  $(\tau_F)_{ref} = 1.6$  ns corresponding to the intrinsic lifetime of the Zn–porphyrin core. The fluorescence lifetimes are summarized in Table 3.

The decay rate of the Zn–porphyrin fluorescence in dendrimer-1 increases with the solvent polarity (Figure 6b). Importantly, the decay curves of dendrimer-1 are best curve-fitted as a bi-exponential function in all solvents; the contribution of the fast-decaying component increases with the solvent polarity. The slower-decaying component in dendrimer-1 has a lifetime that is comparable to that observed for dendron-3, except for the value in 1,4-dioxane.

In order to reveal the ET kinetics in more quantitative detail, we evaluated the rate constants for the CS ( $k_{CS}$ ) via the excited singlet state of Zn–porphyrin using eq 1, where  $(\tau_F)_{ref}$  is a lifetime (1.6 ns) of dendrimer-2;

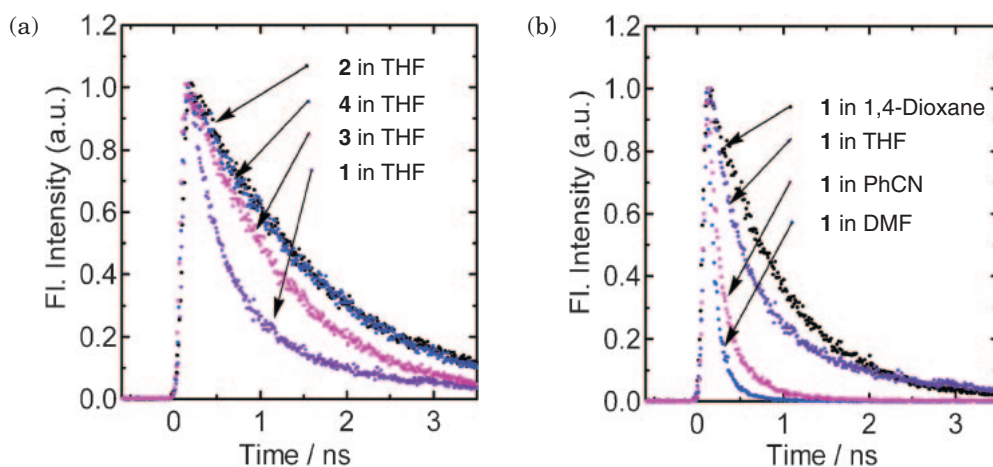


**Figure 6.** (a) Fluorescence decays of **1–4** in the 600–660 nm range with  $\lambda_{\text{ex}} = 410$  nm in THF. (b) Fluorescence decays of dendrimer-**1** in the 610–660 nm range with  $\lambda_{\text{ex}} = 410$  nm in various solvents.

**Table 3.** Fluorescence Lifetimes ( $\tau_{\text{F}}$ ) of Zn–Porphyrin Core

Compds	$\tau_{\text{F}}$ /ns (fraction)			
	1,4-Dioxane	THF	Benzonitrile	DMF
<b>1</b> <sup>a)</sup>	0.73 (35%)	0.32 (63%)	0.16 (88%)	0.11 (92%)
	1.21 (65%)	1.20 (37%)	0.55 (12%)	0.43 (8%)
<b>2</b>	1.70 (100%)	1.60 (100%)	1.60 (100%)	1.60 (100%)
<b>3</b>	1.81 (100%)	1.10 (100%)	0.46 (100%)	0.37 (100%)
<b>4</b>	1.71 (100%)	1.60 (100%)	0.90 (100%)	0.76 (100%)

a) Double-exponential decay was observed.

$$k_{\text{CS}} = (1/\tau_{\text{F}})_{\text{sample}} - (1/\tau_{\text{F}})_{\text{ref}} \quad (1)$$

The  $k_{\text{CS}}$  values are summarized in Table 4. Dendrimer-**1** has two  $k_{\text{CS}}$  values corresponding to the two lifetimes (Table 3). The  $k_{\text{CS}}$  values for dendron-**3** and dyad-**4** in 1,4-dioxane and for dyad-**4** in THF are too small to be accurately determined.

The  $k_{\text{CS}}$  values for dendrimer-**1** are strongly solvent-polarity dependent; the value in DMF is almost 10 times larger than that in 1,4-dioxane in both fast and slow components. The weighted average  $(k_{\text{CS}})_{\text{w}}$  for dendrimer-**1** is calculated as  $0.43 \times 10^9 \text{ s}^{-1}$  in 1,4-dioxane,  $1.7 \times 10^9 \text{ s}^{-1}$  in THF,  $5.2 \times 10^9 \text{ s}^{-1}$  in benzonitrile, and  $8.1 \times 10^9 \text{ s}^{-1}$  in DMF. Using the standard decay rate constant of  $0.63 \times 10^9 \text{ s}^{-1}$  (for dendrimer-**2**), the quenching efficiencies due to ET that is calculated as  $(k_{\text{CS}})_{\text{w}} / ((k_{\text{CS}})_{\text{w}} + 0.63 \times 10^9)$  increase with solvent polarity; they become 38% in 1,4-dioxane, 73% in THF, 89% in benzonitrile, and 93% in DMF, as listed in Table 2. These quenching efficiencies are roughly comparable to the steady-state fluorescence quenching efficiencies shown in Table 2.

**Table 4.** Charge-Separation Rate Constants ( $k_{\text{CS}}$ ) from Excited Singlet State of Zn–Porphyrin to AQ-Terminal in Dendrimer-**1**

Compds	$k_{\text{CS}}/\text{s}^{-1}$ <sup>a)</sup>			
	1,4-Dioxane	THF	Benzonitrile	DMF
<b>1</b>	$0.782 \times 10^9$ (35%)	$2.50 \times 10^9$ (63%)	$5.74 \times 10^9$ (88%)	$8.63 \times 10^9$ (92%)
	$0.238 \times 10^9$ (65%)	$0.208 \times 10^9$ (37%)	$1.19 \times 10^9$ (12%)	$1.70 \times 10^9$ (8%)
<b>3</b>	—	$0.284 \times 10^9$	$1.55 \times 10^9$	$2.08 \times 10^9$
<b>4</b>	—	—	$0.486 \times 10^9$	$0.691 \times 10^9$

a) Fluorescence lifetimes of dendrimer-**2** were used as a standard ( $\tau_{\text{F}})_{\text{ref}}$ .

In a polar solvent, the  $k_{\text{CS}}$  value increases in the order of dyad-**4** < dendron-**3** < dendrimer-**1** (for the fast and major component). The  $k_{\text{CS}}$  value for dendrimer-**1** in DMF is almost 12 times faster than that of dyad-**4**, demonstrating this advantage of the dendrimer structure (dendrimer effect on ET) for the CS process from  $^1\text{Zn-porphyrin}^*$  to the AQ-terminal through the EtPh conjugate chain (Figure 7). This is the first set of experimental data that clearly establishes how the dendrimer architecture is relevant to the ET process of the incorporated donor–conjugate bridge–acceptor system.

**Modeling Study of dyad-4.** The constant D–A distance, similar redox values, and similar excitation energy in encapsulated dendron-**3**, uncovered dyad-**4**, and dendrimer-**1** suggest a minor role of the free energy term in the difference in the electron-transfer rate in these compounds, but they also indicate the importance of the electronic coupling matrix in the Marcus equation. In addition, the presence of conformational isomers (probably rotamers around ethynylene bonds), particularly for dendrimer-**1** in polar solvents, is suggested in the following experiments: 1) the  $^1\text{H NMR}$  study indicates a relatively slow conformational isomerism at room temperature in dendrimer-**1**, 2) a UV–vis spectral study reveals a CT-type broadening of the Soret band of dendrimer-**1** in polar solvents, and 3) a dynamic fluorescence quenching study clearly shows the presence of fast- and slow-decaying components, with the former becoming predominant in polar solvents. These results suggest that the fast and major isomer (rotamer) in polar solvents exhibits a broad Soret band, and that the structure of the rotamers definitely affects the electronic interactions in the ET process.

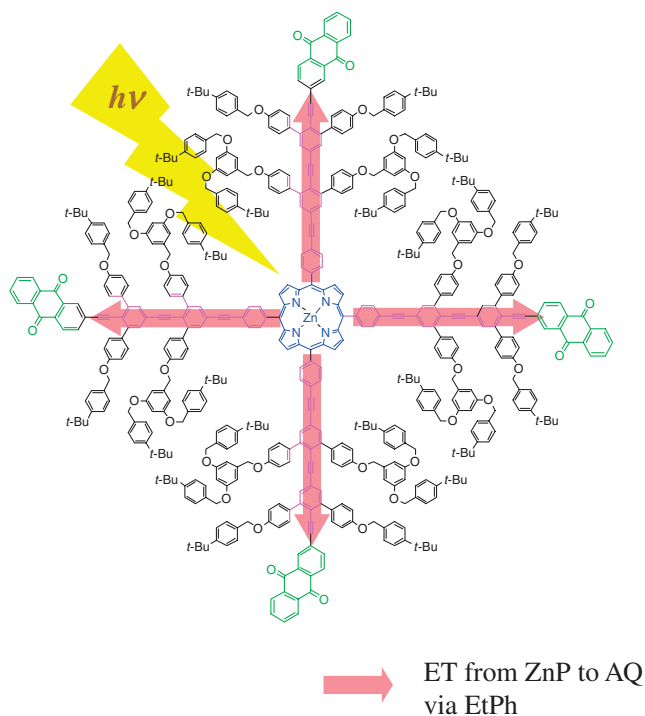


**Figure 7.** Schematic illustration of dendrimer effect on ET in dendrimer-1 showing ET from the Zn-porphyrin core to AQ terminals by excitation of Zn-porphyrin.

In order to gain insight into the relationship between the structures and energies of the rotamers in the present system, a conformational analysis of dyad-4 was carried out by using MO calculations. The structures were optimized using Spartan (AM1 method) with fixed dihedral angles ( $0$  or  $90^\circ$  for the phenyl rings A, B, C, and D). The dihedral angle between Zn-porphyrin and phenyl ring A was also fixed at  $90^\circ$  for the sake of simplicity, even though this dihedral angle is typically  $65\text{--}80^\circ$  according to crystal structure analysis.<sup>24</sup> The energy of the AM1-optimized structure was recalculated using Gaussian program (B3LYP/6-31G(d)).<sup>25</sup> Figure 8 shows the structures and energies (B3LYP/6-31G(d)//AM1) of the eight possible conformers of dyad-4. The most stable Conf 1 is a global energy minimum structure, while the other structures (Conf 2–Conf 8) are energy maxima, from which energy barriers of bond rotation can be estimated. The relative energies of these rotamers (Conf 1–8) are within  $16\text{ kJ mol}^{-1}$ , which indicates very rapid rotation of these rings at room temperature. Their stability generally increases in longer conjugation, as shown in Figure 8-I. At the same conjugation length, AQ-containing conjugations tend to provide a higher degree of stability.

The conformers of intermediate dihedral angles between rings A–D have intermediate energies. Therefore, the energies of these conformers may be altered by a small perturbation. This consideration is in agreement with experimentally derived results for the structures of widely investigated unsubstituted and alkyl-substituted EtPh-type compounds,<sup>26–29</sup> which show a stability of planar forms, even though the barriers to rotation of phenylene groups are low, which are also dependent on subtle changes in the environments.<sup>30</sup>

### Dendrimer Effect and Mechanism of Electron Transfer.

Because of the similarity of their electrochemical parameters, the differences in the  $k_{\text{CS}}$  values among dendrimer-1, dendron-3, and dyad-4 can most likely be ascribed to the electronic interaction between  $^1\text{Zn-porphyrin}^*$  and AQ-moieties. According to the general principle of electronic interaction in photoinduced ET, an important orbital interaction in the ET that includes an excited electron donor and a ground state acceptor must be the interaction between the  $\text{LUMO}_{\text{donor}}$  and the  $\text{LUMO}_{\text{acceptor}}$ .<sup>31</sup> Then, the differences in  $k_{\text{CS}}$  value may be attributed to the orbital interaction between the donor  $\pi^*_{\text{Por}}$  (porphyrin) orbital and the  $\pi^*_{\text{AQ}}$  (AQ) acceptor orbital through the spacer  $\sigma$ -orbitals or twisted  $\pi$ -orbitals of the ring A. Conf 1 (Figure 8-I) has a coplanar relation between rings A, B, and C; thus,  $\pi^*_{\text{AQ}}$  extends to ring A (Figure 8-II, right-upper MO). Although the extended  $\pi^*_{\text{AQ}}$  is perpendicular to  $\pi^*_{\text{Por}}$ , the electron transfer would readily occur, as has been experimentally shown in highly twisted short-linked donor\*–acceptor type dyads.<sup>32</sup> In addition, the torsion angle between the porphyrin ring and ring A is not exactly perpendicular, but is  $65\text{--}80^\circ$ ,<sup>24</sup> which allows for a direct  $\pi$ – $\pi$  type molecular orbital interaction that results in fast ET. In Conf 2, which has a parallel orientation between the porphyrin ring and the AQ ring separated by a twisted ring A,  $\pi^*_{\text{Por}}$  interacts with the  $\sigma$ -bond orbital  $\sigma_{\text{ringA}}$  to give hybrid  $\pi^*_{\text{Por}}-a\sigma_{\text{ringA}}$  ( $0 < a \ll 1$ ) orbital (Figure 8-II, left MO), whereas  $\pi^*_{\text{AQ}}$  can also interact with  $\sigma_{\text{ringA}}$  to provide hybrid  $\pi^*_{\text{AQ}}-b\sigma_{\text{ringA}}$  ( $0 < b \ll 1$ ) orbital (Figure 8-II, right-lower MO). The  $\sigma$ -mixing can be visible in the LUMOs of the model donor (Conf 2-D-LUMO) and the model acceptor (Conf 2-A-LUMO) (Figure 8-II). Alternatively, direct molecular orbital interaction is also possible between  $\pi^*_{\text{Por}}$  and  $\pi^*_{\text{AQ}}$  due to the loose torsion angle ( $65\text{--}80^\circ$ ) between the porphyrin ring and the phenyl ring A, which facilitates ET from  $^1\text{Zn-porphyrin}^*$  to AQ. A similar consideration is also possible for the conformers of parallel orientation (Conf 3, 4, and 8). They have higher energies and  $\sigma$ -orbitals of longer sizes, however, which decrease their contribution to the ET process.

Dendron-3 decays 3 times faster than the uncovered dyad-4 in polar solvents. The fluorescence intensities of dendron-3 and dyad-4 decay with single exponential, and there is no evidence for the participation of rotamers in the ET in dendron-3. The faster rate of decay in dendron-3 may be attributed to a subtle change in electronic perturbation caused by the introduction of BE chains, i.e., the introduction of electron-donating BE chains to the EtPh groups would increase the energy level of  $\pi^*_{\text{AQ}}$ , leading to a stronger orbital interaction between the  $\pi^*_{\text{Por}}$  orbital and  $\pi^*_{\text{AQ}}$  orbital to give a faster ET. We assume that dendron-3 and dyad-4 undergo ET via the same rotamer, essentially the one which has the most stable conformation, Conf 1.

On the other hand, dendrimer-1 exhibits a fluorescence decay of double-exponential functions, and the rapidly decaying components are 4–5 times faster than those of dendron-3. The fast-decaying component is predominant in polar solvents. Importantly, the slower component decays at a rate constant that is similar to that of dendron-3.  $^1\text{H NMR}$  and stationary fluorescence studies also indicate the presence of conformational isomers. We propose the structures **1-A** and **1-B** for dendrimer-1 (Chart 2). The conformer **1-A** has a partial

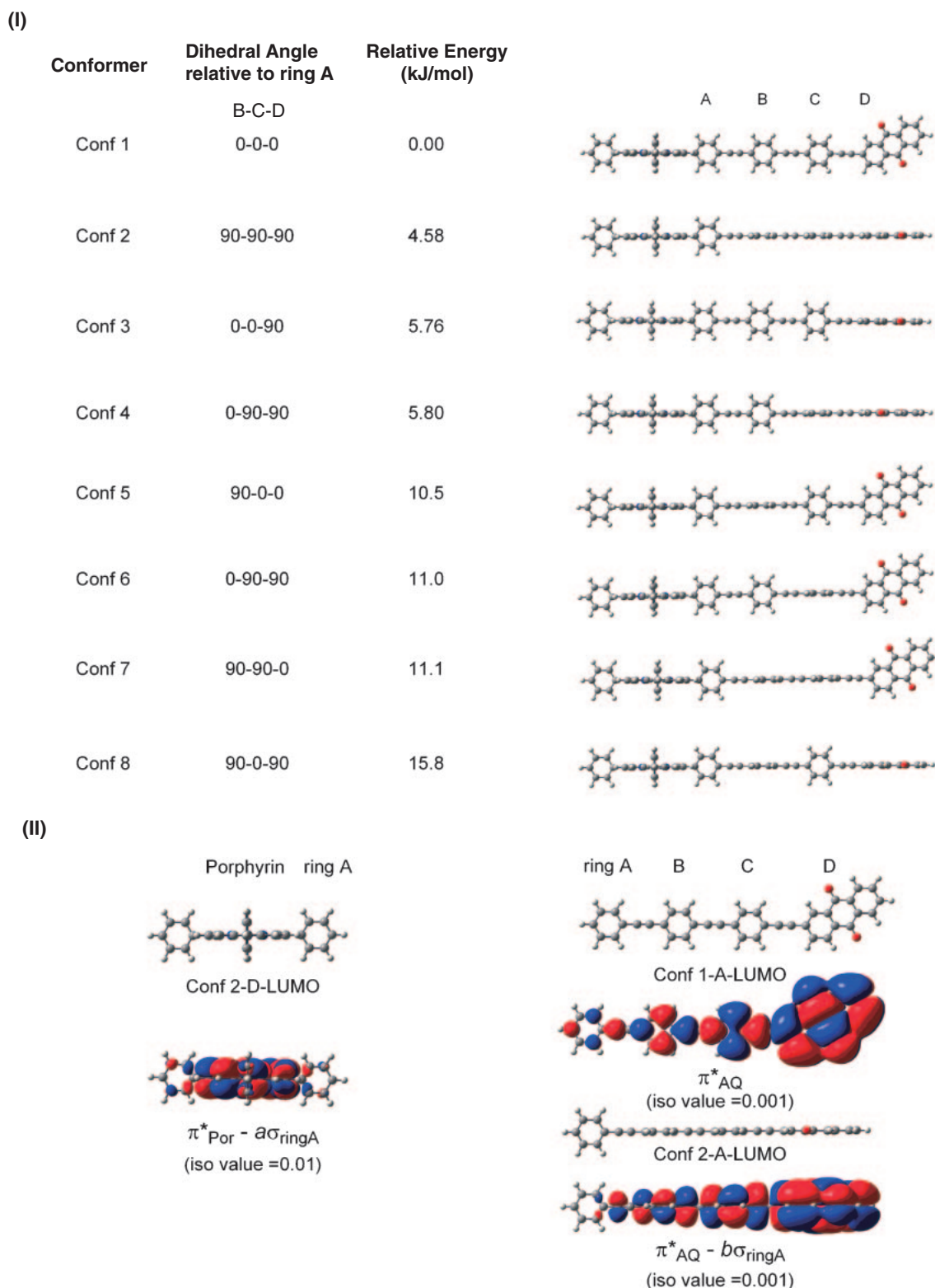


**Figure 8.** Structures and relative energies of the eight possible conformers of dyad-4 (I) and the LUMOs of the model donor and acceptor in Conf 1 and 2 (II).

conformation similar to that of dendron-3 (Conf 1) and each dendron has a large enough space to behave independently. Under this condition, the  $k_{CS}$  value would not be much different with dendron-3. On the other hand, the conformer **1-B** has a flat conformation (Conf 2 or its analog) between the Zn-porphyrin

ring and the EtPh moiety separated by the phenyl ring A with a torsion angle of  $65\text{--}80^\circ$  toward the Zn-porphyrin ring.<sup>24</sup> This partially overlapping orientation would facilitate the electron transfer. The preference of flat conformation **1-B** over **1-A** particularly in polar solvents, can be ascribed to the hydro-

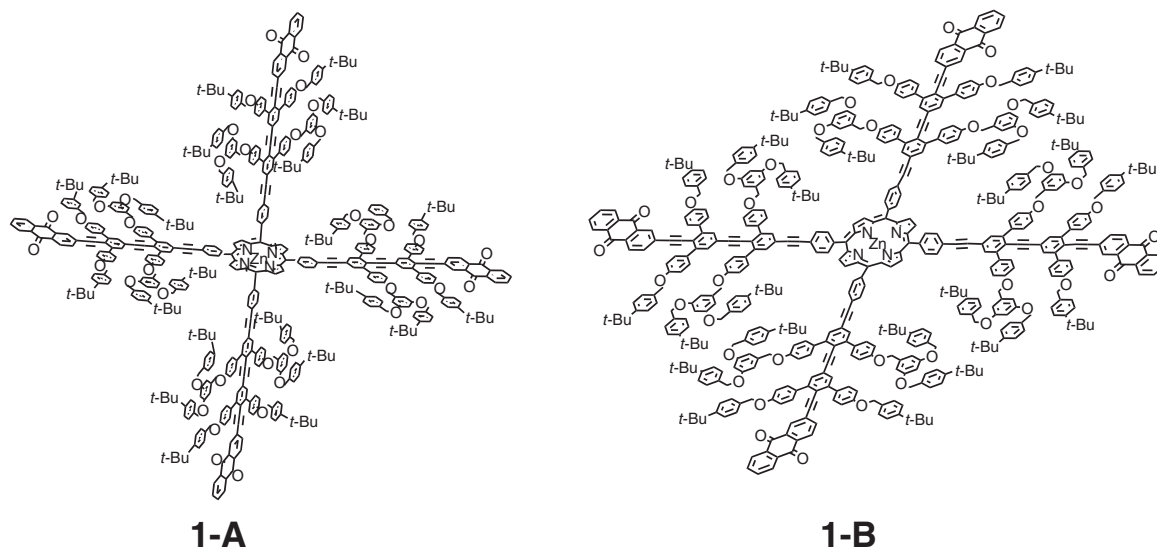


Chart 2. Proposed conformers for conformer-1-A and 1-B.

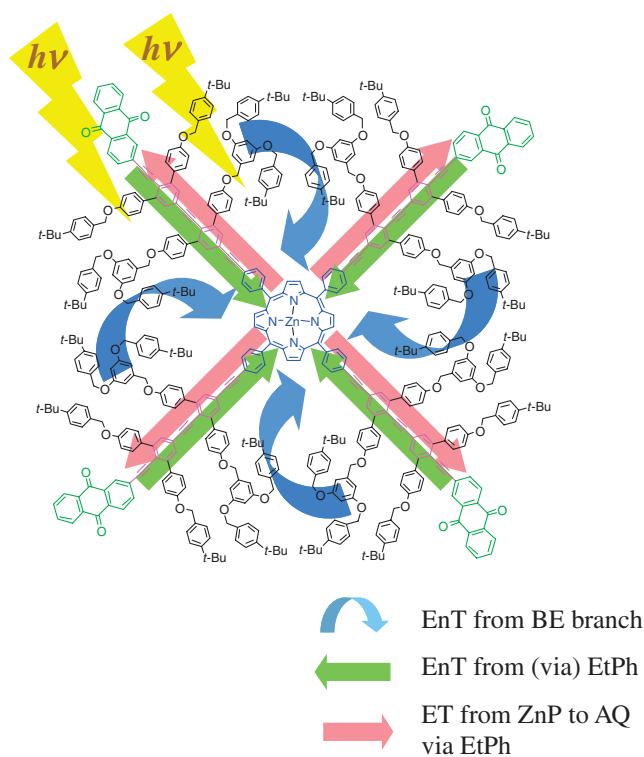


Figure 9. Schematic illustration of photoinduced processes obtained by the combination of EnT and ET in dendrimer-1.

phobic interactions of dendrons within dendrimer-1. Such a hydrophobic interaction in polar solvents has been well documented in the literature.<sup>33</sup> Furthermore, Aida and co-workers have reported that van der Waals interactions between the large dendritic wedges enforce the planar conformation on linear conjugated chains.<sup>34</sup> A similar attractive interaction operates cooperatively between the dendron units in dendrimer-1 to produce the stable planar conformer (1-B). The interchange of the two conformations between 1-B and 1-A would be energetically and entropically slow because of the processes

that involve many bulky BE chains. This is compatible with the fact that broader signals in the <sup>1</sup>H NMR spectra were observed for dendrimers 1 and 2 but not for dendron-3. Further, this partially overlapping flat conformation would permit electronic communications between Zn-porphyrin and the four AQ groups, even in the ground state, as observed in UV-vis spectra in polar solvents. The larger  $k_{CS}$  value of 1-B as opposed to 1-A can probably be attributed to this weak conjugation between <sup>1</sup>ZnTPP\* and the four AQ rings within the flat conformation induced by the hydrophobic interactions of BE chains.

### Conclusion

In summary, the ET and EnT of snowflake-shaped Zn-porphyrin dendrimers with AQ and phenyl terminals (dendrimer-1 and dendrimer-2, respectively) were mainly investigated by means of time-resolved fluorescence measurements. Highly efficient (ca. 100%) intramolecular EnT from dendron moieties (BE branches and/or EtPh chains) to the Zn-porphyrin core was observed in the snowflake-shaped dendrimer-2 with phenyl terminals. The EtPh conjugated chain was found to play an important role as a mediator for the efficient EnT (dendrimer effect on EnT), which facilitates the design of larger functional antenna systems with the dendrimer architecture.

The accumulated excited energy to the Zn-porphyrin core can be used as a chemical potential by replacing the phenyl groups with the AQ groups. Thus, the quenching rates of charge separation ( $k_{CS}$ ) of dendrimer-1 and the BE-covered dendron-3 were compared by means of dynamic fluorescence lifetime shortening. Dendrimer-1 showed the fastest charge separation rate. The  $k_{CS}$  values increased in the order of  $4 < 3 < 1$  in all the solvents examined. The order of  $4 < 3 < 1$  may be attributed to the substituent effect of BE branches on the EtPh chain. The order  $3 < 1$  can be explained by a cooperative effect of the conformational change induced by the inter-dendron type hydrophobic interaction of BE chains and  $\pi$ -conjugation between Zn-porphyrin and the four AQ groups (the dendrimer effect on ET). The photoinduced EnT and ET are summarized in Figure 9.

These dendrimer effects establish the fact that snowflake-type dendrimers are extremely valuable for efficient light harvesting motifs as well as fast charge separation. Further studies for the construction of light-emitting devices using these dendrimer effects on EnT and artificial photosynthetic models that employ an efficient charge separation process (the dendrimer effect on ET) are currently in progress in our laboratory.

### Experimental

**General.** Melting points were taken on a Yanako MP J-3 and are uncorrected.  $^1\text{H}$ NMR spectra were recorded on a JEOL Lambda 300, 400, and Bruker Avance 600 spectrometers. The JEOL Lambda 400 spectrometer was used for the variable temperature NMR measurement for dendrimers **1** and **2**. Chemical shifts were recorded in units of parts per million downfield from tetramethylsilane as internal standard and all coupling constants are reported in Hz. UV-vis spectra were measured with JASCO/V-570 and Shimadzu UV-2550 spectrophotometers. Steady-state fluorescence spectra were measured with Shimadzu RF-5300 PC and Perkin-Elmer LS50B spectrofluorophotometers. IR spectra were obtained on a Shimadzu FTIR-8700 spectrometer. The mass spectra were recorded on JEOL JMS-700T and JMX-AX500 spectrometers. MALDI-TOF mass was measured on a Shimadzu-Kratos AXIMA-CFR Plus spectrometer using dithranol as a matrix reagent. Elemental analyses were obtained from the Analytical Center in Osaka City University. Redox potentials were measured with a voltammetric analyzer (BAS CV-50W) in a conventional three-electrode-cell equipped with Pt-working and counter electrodes with a SCE reference electrode at a scan rate of  $100\text{ mV s}^{-1}$ . TLC was carried out on 0.2 mm Merck silica gel (60 F<sub>254</sub>) precoated plates. Merck silica gel 60 (0.063–0.200 mm) was used for column chromatography. Recycling preparative HPLC was carried out using a Japan Analytical Industry LC-908 with JAIGEL-1H, -2H, and -2.5H GPC columns. 2-Iodoanthraquinone (**7**),<sup>15</sup> 5,10,15,20-tetrakis(4-ethynylphenyl)porphyrinatozinc(II) (**10**),<sup>16</sup> and 5,15,20-tris(3,5-di-*tert*-butylphenyl)-10-(4-ethynylphenyl)porphyrinatozinc(II) (**14**)<sup>35</sup> were prepared according to the reported methods. The synthesis of dendrons **5**, **11**, and **17** has already been described in our preliminary communication as Supporting Information.<sup>11</sup> Commercially available reagents and solvents were purified and dried when necessary.

#### General Procedure for Sonogashira Coupling Reactions.

Before beginning the reactions, all solid samples were dried in vacuo and THF, triethylamine, and ethyldiisopropylamine were deaerated by bubbling nitrogen or argon. An oven-dried vessel was charged with the aryl iodide, terminal alkyne, bis(triphenylphosphine)palladium(II) dichloride (5 mol %), and copper(I) iodide (10 mol %). The vessel was evacuated and backfilled with nitrogen or argon three times. To the vessel, THF and the amine were added in this order. The mixture was stirred at room temperature or 60 °C. After filtration, the solvent was evaporated and the resulting residue was purified by column chromatography on silica gel. Eluents and other slight modifications are described below for each material.

**General Procedure for the Iodination of Triazenes.** To a thick-walled oven-dried screw cap tube was added the

corresponding triazene, iodine, and iodomethane as the solvent. The tube was flushed with nitrogen, sealed and heated at 80 °C overnight. The reaction mixture was cooled to room temperature and diluted with dichloromethane. The mixture was washed with sodium thiosulfate solution and brine and dried over sodium sulfate. After filtration the solvent was evaporated. The resulting solid was filtered through a plug of silica gel with dichloromethane. After evaporation of the solvent in vacuo, a pure product was obtained by recrystallization.

**General Procedure for Desilylation.** To the solution of silylated alkyne (1.00 mmol) in THF (20 mL) was added TBAF (THF solution, 1.2 mL, 1.2 mmol). The mixture was stirred for 0.5 h. After the solvent was removed in vacuo, the residue was passed through a short column of silica gel with dichloromethane. The crude product was purified by recrystallization from hexane–ethyl acetate.

**Dendron 6.** According to the general procedure, dendron **5** (1.91 g, 1.00 mmol) in THF (20 mL) was reacted with TBAF (1.2 mL, 1.2 mmol) to afford dendron **6** (1.56 g, 87%): yellow powder; mp 145.5–146.0 °C;  $^1\text{H}$ NMR (400 MHz,  $\text{CDCl}_3$ ):  $\delta$  7.66 (d,  $J = 8.8$  Hz, 4H), 7.46 (d,  $J = 8.8$  Hz, 4H), 7.44 (s, 2H), 7.40–7.30 (m, 24H), 7.04 (d,  $J = 8.8$  Hz, 4H), 7.03 (s, 2H), 6.95 (d,  $J = 8.8$  Hz, 4H), 6.72 (d,  $J = 2.2$  Hz, 4H), 6.56 (t,  $J = 2.2$  Hz, 2H), 4.97 (s, 4H), 4.96 (s, 8H), 4.85 (s, 4H), 3.78 (q,  $J = 7.1$  Hz, 4H), 2.97 (s, 1H), 1.30 (m, 60H);  $^{13}\text{C}$ NMR (75 MHz,  $\text{CDCl}_3$ ):  $\delta$  160.27, 158.58, 158.27, 150.99, 150.92, 150.85, 145.52, 145.30, 139.44, 134.17, 133.85, 133.71, 132.73, 130.85, 130.54, 130.28, 127.60, 127.56, 125.49, 125.44, 124.19, 120.18, 117.92, 116.13, 114.09, 114.05, 106.19, 101.55, 95.06, 92.60, 84.90, 82.42, 70.00, 69.92, 69.70, 34.55 (2C), 31.32 (2C); IR (KBr): 2960.5(s), 2868.0(m), 1608.5(s), 1506.3(s), 1456.2(s), 1244.0(s), 1155.3(s), 1016.4(m), 831.3(s)  $\text{cm}^{-1}$ ; MS (FAB)  $m/z$  1791 ( $\text{M}^+$ ); Anal. Calcd for  $\text{C}_{124}\text{H}_{131}\text{N}_3\text{O}_8$ : C, 83.14; H, 7.37; N, 2.35%. Found: C, 83.24; H, 7.36; N, 2.41%.

**Dendron 8.** According to the general procedure, dendron **6** (1.25 g, 0.700 mmol), 2-iodoanthraquinone (**7**) (0.260 g, 0.770 mmol), bis(triphenylphosphine)palladium(II) dichloride (44 mg, 0.070 mmol), and copper(I) iodide (27 mg, 0.14 mmol) in ethyldiisopropylamine (10 mL) and THF (10 mL) were reacted at 80 °C overnight. The crude product was purified by column chromatography on silica gel (hexane–dichloromethane 1:1) and recrystallization from toluene to afford dendron **8** (1.20 g, 86%): red powder; mp 227.5–228.5 °C;  $^1\text{H}$ NMR (400 MHz,  $\text{CDCl}_3$ ):  $\delta$  8.29–8.25 (m, 2H), 8.11 (d,  $J = 8.0$  Hz, 1H), 7.97 (d,  $J = 1.7$  Hz, 1H), 7.78–7.76 (m, 2H), 7.67 (d,  $J = 8.6$  Hz, 4H), 7.54 (d,  $J = 8.6$  Hz, 4H), 7.45 (s, 2H), 7.40–7.26 (m, 25H), 7.11 (s, 2H), 7.06 (d,  $J = 8.6$  Hz, 8H), 6.73 (d,  $J = 2.2$  Hz, 4H), 6.57 (t,  $J = 2.2$  Hz, 2H), 4.99 (s, 4H), 4.97 (s, 4H), 4.96 (s, 8H), 3.79 (q,  $J = 7.2$  Hz, 4H), 1.32–1.29 (m, 60H);  $^{13}\text{C}$ NMR (150 MHz,  $\text{CDCl}_3$ ):  $\delta$  182.14, 181.99, 160.29, 158.93, 158.30, 150.93, 150.80, 150.68, 145.39, 144.87, 139.45, 135.47, 134.31, 133.96, 133.90, 133.85, 133.74, 133.39, 133.29, 133.04, 132.62, 131.57, 131.06, 130.80, 130.08, 129.73, 129.50, 127.72, 127.57, 127.09, 126.99, 125.46, 125.41, 124.92, 120.27, 117.95, 116.00, 114.10, 106.02, 101.53, 95.01, 94.98, 94.97, 93.04, 69.92, 69.88 (2C), 34.53 (2C), 31.35, 31.31; IR (KBr): 2960.5(m), 2868.0(w), 1676.0(m), 1593.1(s), 1508.2(s), 1456.2(m),

1244.0(s), 1157.2(s), 1016.4(w), 831.3(m)  $\text{cm}^{-1}$ ; MS (FAB)  $m/z$  1996 ( $\text{M}^+$ ); Anal. Calcd for  $\text{C}_{138}\text{H}_{137}\text{N}_3\text{O}_{10}$ : C, 82.97; H, 6.91; N, 2.10%. Found: C, 83.06; H, 6.89; N, 2.12%.

**Dendron 9.** According to the general procedure, dendron **8** (999 mg, 0.500 mmol) was reacted with iodine (127 mg, 0.500 mmol) in iodomethane (10 mL). The crude product was purified by recrystallization from toluene–hexane to afford dendron **9** (830 mg, 82%): yellow powder; mp 239.5–240.5 °C;  $^1\text{H}$ NMR (400 MHz,  $\text{CDCl}_3$ ):  $\delta$  8.26–8.23 (m, 2H), 8.08 (d,  $J = 8.0$  Hz, 1H), 7.93 (d,  $J = 1.7$  Hz, 1H), 7.77–7.74 (m, 2H), 7.71 (s, 2H), 7.58 (d,  $J = 8.8$  Hz, 4H), 7.49 (d,  $J = 8.8$  Hz, 4H), 7.39–7.26 (m, 25H), 7.08–7.05 (m, 10H), 6.72 (d,  $J = 2.2$  Hz, 4H), 6.56 (t,  $J = 2.2$  Hz, 2H), 4.99 (s, 4H), 4.97 (s, 4H), 4.95 (s, 8H), 1.31–1.29 (m, 54H);  $^{13}\text{C}$ NMR (150 MHz,  $\text{CDCl}_3$ ):  $\delta$  181.89, 181.68, 160.31, 159.01, 158.74, 150.93, 150.78, 145.87, 144.82, 139.17, 136.90, 135.32, 133.89, 133.71, 133.23, 133.16, 132.85, 132.44, 132.39, 131.47, 131.07, 130.83, 130.15, 129.41, 129.38, 127.74, 127.56, 127.01, 126.87, 125.44, 125.39, 124.04, 119.34, 118.56, 114.33, 114.06, 105.91, 101.51, 96.11, 94.91, 94.78, 94.49, 90.95, 69.88, 69.85, 34.53 (2C), 31.35, 31.31; IR (KBr): 2962.5(s), 2868.0(m), 1676.0(m), 1593.1(s), 1508.2(s), 1456.2(m), 1282.6(s), 1155.3(s), 1016.4(m), 831.3(s)  $\text{cm}^{-1}$ ; MS (MALDI-TOF)  $m/z$  2045.41 ( $[\text{M} + \text{Na}]^+$ ) (Calcd for  $\text{C}_{134}\text{H}_{127}\text{IO}_{10}\text{Na}$ : 2045.84); Anal. Calcd for  $\text{C}_{134}\text{H}_{127}\text{IO}_{10}$ : C, 79.50; H, 6.32%. Found: C, 79.62; H, 6.30%.

**Dendrimer-1.** According to the general procedure, dendron **9** (425 mg, 0.210 mmol) was reacted with porphyrin **10** (38.7 mg, 0.050 mmol) in the presence of bis(triphenylphosphine)palladium(II) dichloride (12.6 mg, 0.020 mmol), and copper(I) iodide (7.6 mg, 0.040 mmol) in ethyldiisopropylamine (10 mL) and THF (20 mL) at 80 °C for 4 days. After addition of bis(triphenylphosphine)palladium(II) dichloride (12.6 mg, 0.020 mmol), and copper(I) iodide (7.6 mg, 0.040 mmol), the mixture was stirred 80 °C for 3 days. The crude product was purified by column chromatography on silica gel (dichloromethane–hexane 4:1) and recycling preparative HPLC (chloroform) to afford dendrimer-**1** (150 mg, 36%). Analytical sample was obtained by recrystallization from toluene–acetonitrile: brown solid; mp >300 °C;  $^1\text{H}$ NMR (400 MHz, tetrachloroethane- $d_2$ , 135 °C):  $\delta$  8.96 (s, 8H), 8.25–8.19 (s, 16H), 8.09 (d,  $J = 8.0$  Hz, 4H), 7.95–7.92 (m, 12H), 7.73–7.68 (m, 32H), 7.54 (d,  $J = 8.8$  Hz, 16H), 7.35–7.27 (m, 100H), 7.14 (s, 8H), 7.11–7.06 (m, 32H), 6.72 (d,  $J = 2.2$  Hz, 16H), 6.58 (t,  $J = 2.2$  Hz, 8H), 4.97 (s, 16H), 4.94 (s, 16H), 4.91 (s, 32H), 1.31–1.29 (m, 216H); IR (KBr): 3400.3(bw), 2962.5(s), 2868.0(w), 1676.0(m), 1606.6(s), 1593.1(s), 1506.3(s), 1458.2(m), 1284.5(m), 1245.9(m), 1155.3(m), 1016.4(m), 831.3(m)  $\text{cm}^{-1}$ ; MS (MALDI-TOF)  $m/z$  8357.04; Anal. Calcd for  $\text{C}_{588}\text{H}_{532}\text{N}_4\text{O}_{40}\text{Zn}$ : C, 84.48; H, 6.41; N, 0.67%. Found: C, 84.37; H, 6.17; N, 0.72%.

**Dendrimer-2.** According to the general procedure, dendron **11** (265 mg, 0.17 mmol) was reacted with porphyrin **10** (31 mg, 0.040 mmol) in the presence of bis(triphenylphosphine)palladium(II) dichloride (10 mg, 0.016 mmol), and copper(I) iodide (6.0 mg, 0.032 mmol) in ethyldiisopropylamine (10 mL) and THF (10 mL) at 80 °C for 3 days. After addition of bis(triphenylphosphine)palladium(II) dichloride (10 mg, 0.016 mmol) and copper(I) iodide (6.0 mg, 0.032 mmol), the mixture was stirred

80 °C for 2 days. The crude product was purified by column chromatography on silica gel (dichloromethane) and recycling preparative HPLC (chloroform) to afford dendrimer-**2** (107 mg, 41%): dark green solid; mp 300 °C;  $^1\text{H}$ NMR (400 MHz, tetrachloroethane- $d_2$ , 80 °C):  $\delta$  8.99 (s, 8H), 8.23 (d,  $J = 8.5$  Hz, 8H), 7.96 (d,  $J = 8.5$  Hz, 8H), 7.73–7.70 (m, 24H), 7.56 (d,  $J = 8.8$  Hz, 16H), 7.39–6.98 (m, 180H), 6.73 (d,  $J = 2.2$  Hz, 16H), 6.57 (t,  $J = 2.2$  Hz, 8H), 5.01 (s, 48H), 4.98 (s, 16H); IR (KBr): 3031.9(w), 2868.0(w), 1606.6(s), 1506.3(s), 1454.2(m), 1377.1(w), 1292.2(m), 1242.1(s), 1157.2(s), 1026.1(m), 999.1(w), 827.4(m), 734.8(m), 696.3(m)  $\text{cm}^{-1}$ ; MS (MALDI-TOF)  $m/z$  6492.4233; Anal. Calcd for  $\text{C}_{460}\text{H}_{332}\text{N}_4\text{O}_{32}\text{Zn}$ : C, 85.09; H, 5.15; N, 0.86%. Found: C, 85.14; H, 5.11; N, 0.90%.

**Dendron 12.** According to the general procedure, the reaction of dendron **5** (95.3 mg, 0.050 mmol) with iodine (12.7 mg, 0.050 mmol) in iodomethane (1.0 mL) afforded dendron **12** (58 mg, 60%): white solid; mp 207.0–208.0 °C;  $^1\text{H}$ NMR (400 MHz,  $\text{CDCl}_3$ ):  $\delta$  7.71 (s, 2H), 7.58 (d,  $J = 8.8$  Hz, 4H), 7.44 (d,  $J = 8.8$  Hz, 4H), 7.40–7.27 (m, 24H), 7.03 (d,  $J = 8.8$  Hz, 4H), 7.01 (s, 2H), 6.92 (d,  $J = 8.8$  Hz, 4H), 6.71 (d,  $J = 2.2$  Hz, 4H), 6.56 (t,  $J = 2.2$  Hz, 2H), 4.97 (s, 4H), 4.96 (s, 8H), 4.86 (s, 4H), 1.30 (s, 54H), 0.69 (s, 9H), –0.15 (s, 6H);  $^{13}\text{C}$ NMR (75 MHz,  $\text{CDCl}_3$ ):  $\delta$  160.29, 158.67, 158.51, 151.02, 150.86, 146.12, 145.02, 139.25, 136.70, 133.95, 133.69, 132.72, 132.26, 130.75, 130.59, 130.19, 127.57, 127.42, 125.51, 125.45, 122.93, 119.95, 119.71, 114.29, 114.04, 106.17, 104.38, 101.92, 101.54, 96.80, 94.46, 90.73, 69.99, 69.94, 69.72, 34.56, 34.54, 31.33, 25.93, 16.52, –5.06; IR (KBr): 2960.5(m), 2868.0(w), 1608.5(s), 1508.2(s), 1456.2(m), 1245.9(m), 1159.1(m), 1016.4(m), 827.4(s)  $\text{cm}^{-1}$ ; MS (FAB)  $m/z$  1931 ( $\text{M}^+$ ); Anal. Calcd for  $\text{C}_{126}\text{H}_{135}\text{IO}_8\text{Si}$ : C, 78.31; H, 7.04%. Found: C, 78.43; H, 7.07%.

**Dendron 14.** According to the general procedure, dendron **12** (290 mg, 0.15 mmol) was reacted with porphyrin **13** (171 mg, 0.165 mmol) in the presence of bis(triphenylphosphine)palladium(II) dichloride (9.5 mg, 0.015 mmol) and copper(I) iodide (5.7 mg, 0.03 mmol) in ethyldiisopropylamine (1.5 mL) and THF (6.0 mL) at room temperature overnight. The crude product was purified by column chromatography on silica gel (hexane–dichloromethane 3:2) to afford dendron **14** (394 mg, 90%): purple solid; mp 153–154 °C;  $^1\text{H}$ NMR (400 MHz,  $\text{CDCl}_3$ ):  $\delta$  9.01 (d,  $J = 4.4$  Hz, 6H), 8.96 (d,  $J = 4.4$  Hz, 2H), 8.24 (d,  $J = 8.0$  Hz, 2H), 8.09 (m, 6H), 7.93 (d,  $J = 8.0$  Hz, 2H), 7.79 (m, 3H), 7.71 (d,  $J = 8.6$  Hz, 4H), 7.69 (s, 2H), 7.48 (d,  $J = 8.6$  Hz, 4H), 7.40–7.30 (m, 24H), 7.10 (d,  $J = 8.6$  Hz, 4H), 7.08 (s, 2H), 6.94 (d,  $J = 8.6$  Hz, 4H), 6.74 (d,  $J = 2.0$  Hz, 4H), 6.58 (t,  $J = 2.0$  Hz, 2H), 5.01 (s, 4H), 4.97 (s, 8H), 4.87 (s, 4H), 1.53 (m, 54H), 1.31 (m, 54H), 0.71 (s, 9H), –0.13 (s, 6H); IR (KBr): 2962.5(s), 2868.0(m), 1595.0(m), 1506.3(s), 1458.1(m), 1363.6(m), 1247.9(m), 1153.4(m), 1002.9(m), 827.4(m)  $\text{cm}^{-1}$ ; MS (FAB)  $m/z$  2840 ( $\text{M}^+$ ); HRMS (FAB)  $m/z$  calcd for  $\text{C}_{196}\text{H}_{210}\text{N}_4\text{O}_8\text{SiZn}$ : 2839.5209, found: 2839.5249.

**Dendron 15.** According to the general procedure, dendron **14** (380 mg, 0.13 mmol) in THF (20 mL) was reacted with TBAF (0.16 mL, 0.16 mmol) for 15 min to afford dendron **15** (340 mg, 96%): purple solid; mp 163–164 °C;  $^1\text{H}$ NMR (400 MHz,  $\text{CDCl}_3$ ):  $\delta$  9.01 (d,  $J = 4.4$  Hz, 6H), 8.96 (d,  $J = 4.4$  Hz, 2H), 8.24 (d,  $J = 8.0$  Hz, 2H), 8.09 (m, 6H), 7.93 (d,  $J = 8.0$  Hz, 2H), 7.79 (m, 3H), 7.71 (d,  $J = 8.8$  Hz, 4H),

7.69 (s, 2H), 7.48 (d,  $J = 8.8$  Hz, 4H), 7.40–7.32 (m, 24H), 7.10 (d,  $J = 8.8$  Hz, 4H), 7.08 (s, 2H), 6.98 (d,  $J = 8.8$  Hz, 4H), 6.74 (d,  $J = 2.2$  Hz, 4H), 6.57 (t,  $J = 2.2$  Hz, 2H), 5.01 (s, 4H), 4.97 (s, 8H), 4.87 (s, 4H), 3.01 (s, 1H), 1.52 (m, 54H), 1.31 (m, 54H);  $^{13}\text{C}$  NMR (100 MHz,  $\text{CDCl}_3$ ):  $\delta$  160.31, 158.69, 158.61, 151.03, 150.97, 150.53, 150.43, 150.41, 149.76, 148.57, 148.54, 145.47, 145.01, 143.47, 141.78, 139.34, 134.44, 133.86, 133.72, 133.13, 132.62, 132.47, 132.31, 132.20, 131.44, 131.07, 130.89, 130.57, 129.90, 129.66, 129.59, 129.01, 128.20, 127.62, 127.57, 125.51, 125.47, 123.60, 123.36, 122.76, 122.57, 122.17, 120.82, 120.06, 119.69, 118.62, 114.36, 114.15, 106.23, 101.60, 96.99, 91.60, 90.15, 85.28, 82.33, 70.05, 69.96, 69.75, 35.04, 34.57, 31.76, 31.35, 31.34; IR (KBr): 2962.5(s), 2868.0(m), 1595.0(s), 1506.3(s), 1458.1(m), 1363.6(m), 1247.9(m), 1151.4(m), 1002.9(m), 831.3(m)  $\text{cm}^{-1}$ ; MS (FAB)  $m/z$  2725 ( $\text{M}^+$ ); HRMS (FAB)  $m/z$  calcd for  $\text{C}_{190}\text{H}_{196}\text{N}_4\text{O}_8\text{Zn}$ : 2725.4345, found: 2725.4314.

**Dendron-3.** According to the general procedure, dendron **15** (273 mg, 0.10 mmol) was reacted with 2-iodoanthraquinone (**7**) (33 mg, 0.10 mmol) in the presence of bis(triphenylphosphine)palladium(II) dichloride (6.3 mg, 0.010 mmol), and copper(I) iodide (3.8 mg, 0.020 mmol) in ethyldiisopropylamine (1.0 mL) and THF (5.0 mL) at room temperature overnight. The crude product was purified by column chromatography on silica gel (hexane–dichloromethane 1:1) to afford dendron-**3** (229 mg, 78%): brown solid; mp 240–241 °C;  $^1\text{H}$  NMR (400 MHz,  $\text{CDCl}_3$ ):  $\delta$  9.01 (d,  $J = 4.6$  Hz, 6H), 8.96 (d,  $J = 4.6$  Hz, 2H), 8.30–8.27 (m, 2H), 8.24 (d,  $J = 7.8$  Hz, 2H), 8.14 (d,  $J = 7.8$  Hz, 1H), 8.09 (m, 6H), 8.00 (m, 1H), 7.94 (d,  $J = 7.8$  Hz, 2H), 7.80 (m, 5H), 7.73 (d,  $J = 8.6$  Hz, 4H), 7.70 (s, 2H), 7.58 (d,  $J = 8.6$  Hz, 4H), 7.41–7.32 (m, 25H), 7.16 (s, 2H), 7.12 (d,  $J = 8.6$  Hz, 4H), 7.09 (d,  $J = 8.6$  Hz, 4H), 6.75 (d,  $J = 2.0$  Hz, 4H), 6.58 (t,  $J = 2.0$  Hz, 2H), 5.03 (s, 4H), 4.99 (s, 8H), 4.98 (s, 4H), 1.53 (m, 54H), 1.32 (s, 18H), 1.30 (s, 36H); IR (KBr): 2962.5(s), 2868.0(m), 1676.0(m), 1593.1(s), 1506.3(s), 1458.1(m), 1363.6(m), 1284.5(m), 1155.3(m), 1002.9(m), 831.3(m)  $\text{cm}^{-1}$ ; MS (FAB)  $m/z$  2931 ( $\text{M}^+$ ); Anal. Calcd for  $\text{C}_{204}\text{H}_{202}\text{N}_4\text{O}_{10}\text{Zn}$ : C, 83.48; H, 6.94; N, 1.91%. Found: C, 83.43; H, 6.98; N, 1.78%.

**Dendron 18.** According to the general procedure, dendron **17** (140 mg, 0.10 mmol) in THF (10 mL) was reacted with TBAF (0.20 mL, 0.20 mmol) for 10 min. The crude product was purified with a short column of silica gel (hexane–dichloromethane 8:2) to afford dendron **18** (99 mg, 80%): purple powder; mp >300 °C;  $^1\text{H}$  NMR (400 MHz,  $\text{CDCl}_3$ ):  $\delta$  9.01 (d,  $J = 4.6$  Hz, 6H), 8.95 (d,  $J = 4.6$  Hz, 2H), 8.24 (d,  $J = 8.2$  Hz, 2H), 8.09 (m, 6H), 7.92 (d,  $J = 8.2$  Hz, 2H), 7.95 (m, 3H), 7.67 (d,  $J = 8.0$  Hz, 2H), 7.59 (d,  $J = 8.0$  Hz, 2H), 7.52 (dd,  $J = 13.0, 8.6$  Hz, 4H), 3.20 (s, 1H), 1.53 (m, 54H); IR (KBr): 2962.5(s), 2868.0(m), 1593.1(s), 1517.9(m), 1363.6(m), 1247.9(m), 1001.0(s), 798.5(m), 717.5(m)  $\text{cm}^{-1}$ ; MS (FAB)  $m/z$  1237 ( $\text{M}^+$ ); HRMS (FAB)  $m/z$  calcd for  $\text{C}_{86}\text{H}_{84}\text{N}_4\text{Zn}$ : 1236.5989, found: 1236.5985.

**Dyad-4.** According to the general procedure, dendron **18** (100 mg, 0.080 mmol) was reacted with 2-iodoanthraquinone (**7**) (27 mg, 0.080 mmol) in the presence of bis(triphenylphosphine)palladium(II) dichloride (5.0 mg, 0.080 mmol) and copper(I) iodide (3.0 mg, 0.016 mmol) in ethyldiisopropylamine (1.0 mL) and THF (6.0 mL) at room temperature overnight. The

crude product was purified by column chromatography on silica gel (hexane–dichloromethane 1:1) to afford dyad-**4** (108 mg, 93%): dark purple powder; mp >300 °C;  $^1\text{H}$  NMR (400 MHz,  $\text{CDCl}_3$ ):  $\delta$  9.02 (d,  $J = 4.9$  Hz, 6H), 8.96 (d,  $J = 4.9$  Hz, 2H), 8.39 (d,  $J = 1.7$  Hz, 1H), 8.27–8.23 (m, 5H), 8.09–8.08 (m, 6H), 7.93 (d,  $J = 8.3$  Hz, 2H), 7.90 (dd,  $J = 8.3, 1.7$  Hz, 1H), 7.80–7.78 (m, 5H), 7.69 (d,  $J = 8.6$  Hz, 2H), 7.62–7.60 (m, 6H), 1.53 (s, 36H), 1.52 (s, 18H); IR (KBr): 2962.5(s), 2868.0(m), 1676.0(m), 1593.1(s), 1506.3(s), 1458.1(m), 1284.5(m), 1363.6(m), 1284.5(m), 1151.4(m), 1002.9(m), 831.3(m)  $\text{cm}^{-1}$ ; MS (FAB)  $m/z$  1443 ( $\text{M}^+$ ); Anal. Calcd for  $\text{C}_{100}\text{H}_{90}\text{N}_4\text{O}_2\text{Zn}$ : C, 83.11; H, 6.28; N, 3.88%. Found: C, 83.24; H, 6.30; N, 3.73%.

**Conformational Analysis.** Conformational analysis was carried out for **4**. The dihedral angles of  $\pi$ -systems around acetylenic bonds were assumed to be 0 or 90°, for the sake of simplicity. Eight possible conformational isomers were generated using Spartan software<sup>23</sup> and the structures were optimized using the AM1 method. The molecular orbitals in Figure 6 were generated with an isovalue of surface = 0.001 in order to show the  $\sigma$ -orbital mixing in  $\pi\tau_{\text{Por}}^*$  and  $\pi\tau_{\text{AQ}}^*$ .

**Estimation of Energy-Transfer Efficiencies.** For the investigation of light-harvesting properties of dendrimer-**2**, absolute quantum yields ( $\Phi_{\text{F}}$ ) of the fluorescence from the porphyrin cope are measured using Hamamatsu photonics C9920 spectrometer. Energy-transfer efficiencies ( $\Phi_{\text{ET}}$ ) are determined as follows:  $\Phi_{\text{ET}} = \Phi_{\text{F}}$  (sensitized excitation)/ $\Phi_{\text{F}}$  (direct excitation).

**Time-Resolved Fluorescence.** The picosecond time-resolved fluorescence spectra were measured using an argon-ion pumped Ti:sapphire laser (Tsunami) and a streak scope (Hamamatsu Photonics). Details of the setup of the experiment are described elsewhere.<sup>36</sup>

This work was partially supported by a Grant-in-Aid for Science Research (No. 19655016) from the Ministry of Education, Culture, Sports, Science and Technology, Japan. We thank for Hamamatsu Photonics K. K. for measurements of fluorescence quantum yields. We also thank Prof. Yoshio Aso (Osaka University) for helpful discussion.

## Supporting Information

Temperature dependence of  $^1\text{H}$  NMR spectra of **1** and **2**. UV–vis absorption of dendrimer-**1** and fluorescence lifetime measurement. This material is available free of charge via the internet: <http://www.csj.jp/journals/bcsj/>.

## References

- a) G. R. Newcome, C. N. Moorefield, F. Vögtle, *Dendrimers and Dendrons: Concepts, Syntheses, Applications*, VCH, Weinheim, Germany, **2001**. b) J. M. J. Fréchet, D. A. Tomalia, *Dendrimers and Other Dendritic Polymers*, John Wiley & Sons, New York, **2002**.
- a) D.-L. Jiang, T. Aida, *Nature* **1997**, *388*, 454. b) D.-L. Jiang, T. Aida, *J. Am. Chem. Soc.* **1998**, *120*, 10895. c) M. Kimura, T. Shiba, M. Yamazaki, K. Hanabusa, H. Shirai, N. Kobayashi, *J. Am. Chem. Soc.* **2001**, *123*, 5636. d) M.-S. Choi, T. Aida, T. Yamazaki, I. Yamazaki, *Chem.—Eur. J.* **2002**, *8*, 2667. e) F. Loiseau, S. Campagna, A. Hameurlaine, W. Dehaen, *J. Am. Chem.*

- Soc.* **2005**, *127*, 11352. f) M. del Rosario Benites, T. E. Johnson, S. Weghorn, L. Yu, P. D. Rao, J. R. Diers, S. I. Yang, C. Kirmaier, D. F. Bocian, D. Holtzen, J. S. Lindsey, *J. Mater. Chem.* **2002**, *12*, 65. g) A. Nakano, A. Osuka, T. Yamazaki, Y. Nishimura, S. Akimoto, I. Yamazaki, A. Itaya, M. Murakami, H. Miyasaka, *Chem.—Eur. J.* **2001**, *7*, 3134. h) W. Maes, W. Dehaen, *Eur. J. Org. Chem.* **2009**, 4719. i) W.-S. Li, T. Aida, *Chem. Rev.* **2009**, *109*, 6047.
- 3 a) C. Devadoss, P. Bharathi, J. S. Moore, *J. Am. Chem. Soc.* **1996**, *118*, 9635. b) J. S. Melinger, Y. Pan, V. D. Kleiman, Z. Peng, B. L. Davis, D. McMorrow, M. Lu, *J. Am. Chem. Soc.* **2002**, *124*, 12002.
- 4 a) B. Rybtchinski, L. E. Sinks, M. R. Wasielewski, *J. Am. Chem. Soc.* **2004**, *126*, 12268. b) J. Qu, N. G. Pschirer, D. Liu, A. Stefan, F. C. D. Schryver, K. Müllen, *Chem.—Eur. J.* **2004**, *10*, 528. c) I. Oesterling, K. Müllen, *J. Am. Chem. Soc.* **2007**, *129*, 4595. d) T. Weil, E. Reuther, K. Müllen, *Angew. Chem., Int. Ed.* **2002**, *41*, 1900. e) J. M. Serin, D. W. Brousmiche, J. M. J. Fréchet, *Chem. Commun.* **2002**, 2605.
- 5 a) R. Sadamoto, N. Tomioka, T. Aida, *J. Am. Chem. Soc.* **1996**, *118*, 3978. b) C. S. Rajesh, G. J. Capitosti, S. J. Cramer, D. A. Modarelli, *J. Phys. Chem. B* **2001**, *105*, 10175. c) G. J. Capitosti, C. D. Guerreo, D. E. Binkley, Jr., C. S. Rajesh, D. A. Modarelli, *J. Org. Chem.* **2003**, *68*, 247. d) A. Nantalaksakul, A. Mueller, A. Klaiherd, C. J. Bardeen, S. Thayumanavan, *J. Am. Chem. Soc.* **2009**, *131*, 2727. e) M.-S. Choi, T. Aida, H. Luo, Y. Araki, O. Ito, *Angew. Chem., Int. Ed.* **2003**, *42*, 4060.
- 6 a) S. L. Gilat, A. Adronov, J. M. J. Fréchet, *Angew. Chem., Int. Ed.* **1999**, *38*, 1422. b) T. H. Ghaddar, J. F. Wishart, D. W. Thompson, J. K. Whitesell, M. A. Fox, *J. Am. Chem. Soc.* **2002**, *124*, 8285.
- 7 a) D. M. Guldi, A. Swartz, C. Luo, R. Gómez, J. L. Segura, N. Martín, *J. Am. Chem. Soc.* **2002**, *124*, 10875. b) K. R. Justin Thomas, A. L. Thompson, A. V. Sivakumar, C. J. Bardeen, S. Thayumanavan, *J. Am. Chem. Soc.* **2005**, *127*, 373. c) A. Nantalaksakul, R. R. Dasari, T.-S. Ahn, R. Al-Kaysi, C. J. Bardeen, S. Thayumanavan, *Org. Lett.* **2006**, *8*, 2981. d) M. Lor, L. Viaene, R. Pilot, E. Fron, S. Jordens, G. Schweitzer, T. Weil, K. Müllen, J. W. Verhoeven, M. Van der Auweraer, F. C. De Schryver, *J. Phys. Chem. B* **2004**, *108*, 10721. e) X. Camps, E. Dietel, A. Hirsch, S. Pyo, L. Echegoyen, S. Hackbarth, B. Röder, *Chem.—Eur. J.* **1999**, *5*, 2362. f) M. Lor, J. Thielemans, L. Viaene, M. Cotlet, J. Hofkens, T. Weil, C. Hampel, K. Müllen, J. W. Verhoeven, M. Van der Auweraer, F. C. De Schryver, *J. Am. Chem. Soc.* **2002**, *124*, 9918. g) K. Albrecht, K. Yamamoto, *J. Am. Chem. Soc.* **2009**, *131*, 2244. h) H. Kawachi, S. Suzuki, M. Kozaki, K. Okada, D.-M. Shafiqul Islam, Y. Araki, O. Ito, K. Yamanaka, *J. Phys. Chem. A* **2008**, *112*, 5878.
- 8 a) R. E. Blankenship, *Molecular Mechanism of Photosynthesis*, Blackwell Science, Oxford, **2002**. b) K. N. Ferreira, T. M. Iverson, K. Manghlaoui, J. Barber, S. Iwata, *Science* **2004**, *303*, 1831.
- 9 a) A. Osuka, N. Tanabe, S. Kawabata, I. Yamazaki, Y. Nishimura, *J. Org. Chem.* **1995**, *60*, 7177. b) W. B. Davis, W. A. Svec, M. A. Ratner, M. R. Wasielewski, *Nature* **1998**, *396*, 60. c) J. M. Tour, A. M. Rawlett, M. Kozaki, Y. Yao, R. C. Jagessar, S. M. Dirk, D. W. Price, M. A. Reed, C.-W. Zhou, J. Chen, W. Wang, I. Campbell, *Chem.—Eur. J.* **2001**, *7*, 5118. d) M. U. Winters, E. Dahlstedt, H. E. Blades, C. J. Wilson, M. J. Frampton, H. L. Anderson, B. Albinsson, *J. Am. Chem. Soc.* **2007**, *129*, 4291. e) F. Giacalone, J. L. Segura, N. Martín, D. M. Guldi, *J. Am. Chem. Soc.* **2004**, *126*, 5340. f) J. M. Tour, M. Kozaki, J. M. Seminario, *J. Am. Chem. Soc.* **1998**, *120*, 8486. g) J. Ikemoto, K. Takimiya, Y. Aso, T. Otsubo, M. Fujitsuka, O. Ito, *Org. Lett.* **2002**, *4*, 309. h) D. L. Allara, T. D. Dunbar, P. S. Weiss, L. A. Bumm, M. T. Cygan, J. M. Tour, W. A. Reinert, Y. Yao, M. Kozaki, L. Jones, *Ann. N.Y. Acad. Sci.* **1998**, 852, 349.
- 10 a) M. Kozaki, K. Okada, *Org. Lett.* **2004**, *6*, 485. b) M. Kozaki, K. Akita, S. Suzuki, K. Okada, *Org. Lett.* **2007**, *9*, 3315. c) M. Kozaki, H. Tujimura, S. Suzuki, K. Okada, *Tetrahedron Lett.* **2008**, *49*, 2931. d) M. Kozaki, A. Uetomo, S. Suzuki, K. Okada, *Org. Lett.* **2008**, *10*, 4477.
- 11 M. Kozaki, K. Akita, K. Okada, *Org. Lett.* **2007**, *9*, 1509.
- 12 N. Miyaura, A. Suzuki, *Chem. Rev.* **1995**, *95*, 2457.
- 13 a) J. S. Moore, E. J. Weinstein, Z. Wu, *Tetrahedron Lett.* **1991**, *32*, 2465. b) Z. Wu, J. S. Moore, *Tetrahedron Lett.* **1994**, *35*, 5539.
- 14 a) K. Sonogashira, Y. Tohda, N. Hagihara, *Tetrahedron Lett.* **1975**, *16*, 4467. b) R. Chinchilla, C. Nájera, *Chem. Rev.* **2007**, *107*, 874.
- 15 R. W. Higgins, C. L. Hilton, S. D. Deodhar, *J. Org. Chem.* **1951**, *16*, 1275.
- 16 K. Onitsuka, H. Kitajima, M. Fujimoto, A. Iuchi, F. Takei, S. Takahashi, *Chem. Commun.* **2002**, 2576.
- 17 a) R.-H. Jin, T. Aida, S. Inoue, *J. Chem. Soc., Chem. Commun.* **1993**, 1260. b) K. W. Pollak, E. M. Sanford, J. M. J. Fréchet, *J. Mater. Chem.* **1998**, *8*, 519.
- 18 a) R. Charvet, D.-L. Jiang, T. Aida, *Chem. Commun.* **2004**, 2664. b) A. S. D. Sandanayaka, Y. Araki, T. Wada, T. Hasobe, *J. Phys. Chem. C* **2008**, *112*, 19209. c) S. Okada, H. Segawa, *J. Am. Chem. Soc.* **2003**, *125*, 2792.
- 19 K. M. Barkigia, L. Chantranupong, K. M. Smith, J. Fajer, *J. Am. Chem. Soc.* **1988**, *110*, 7566.
- 20 a) D. Kuciauskas, S. Lin, G. R. Seely, A. L. Moore, T. A. Moore, D. Gust, T. Drovetskaya, C. A. Reed, P. D. W. Boyd, *J. Phys. Chem.* **1996**, *100*, 15926. b) W.-N. Yen, S.-S. Lo, M.-C. Kuo, C.-L. Mai, G.-H. Lee, S.-M. Peng, C.-Y. Yeh, *Org. Lett.* **2006**, *8*, 4239.
- 21 a) C. B. Gorman, J. C. Smith, *Acc. Chem. Res.* **2001**, *34*, 60. b) K. W. Pollak, J. W. Leon, J. M. J. Fréchet, M. Maskus, H. D. Abruña, *Chem. Mater.* **1998**, *10*, 30.
- 22 a) A. Weller, *Z. Phys. Chem. (Neue Folge)* **1982**, *133*, 93. b) S. Takahashi, K. Nozaki, M. Kozaki, S. Suzuki, K. Keyaki, A. Ichimura, T. Matsushita, K. Okada, *J. Phys. Chem. A* **2008**, *112*, 2533.
- 23 Spartan '08, Wavefunction, Inc., Irvine, CA.
- 24 For example: M. P. Byrn, C. J. Curtis, Y. Hsiou, S. I. Khan, P. A. Sawin, S. K. Tendick, A. Terzis, C. E. Strouse, *J. Am. Chem. Soc.* **1993**, *115*, 9480.
- 25 M. J. Frisch, G. W. Trucks, H. B. Schlegel, G. E. Scuseria, M. A. Robb, J. R. Cheeseman, J. A. Montgomery, Jr., T. Vreven, K. N. Kudin, J. C. Burant, J. M. Millam, S. S. Iyengar, J. Tomasi, V. Barone, B. Mennucci, M. Cossi, G. Scalmani, N. Rega, G. A. Petersson, H. Nakatsuji, M. Hada, M. Ehara, K. Toyota, R. Fukuda, J. Hasegawa, M. Ishida, T. Nakajima, Y. Honda, O. Kitao, H. Nakai, M. Klene, X. Li, J. E. Knox, H. P. Hratchian, J. B. Cross, V. Bakken, C. Adamo, J. Jaramillo, R. Gomperts, R. E. Stratmann, O. Yazyev, A. J. Austin, R. Cammi, C. Pomelli, J. W. Ochterski, P. Y. Ayala, K. Morokuma, G. A. Voth, P. Salvador, J. J. Dannenberg, V. G. Zakrzewski, S. Dapprich, A. D. Daniels, M. C. Strain, O. Farkas, D. K. Malick, A. D. Rabuck, K. Raghavachari, J. B. Foresman, J. V. Ortiz, Q. Cui, A. G. Baboul, S. Clifford, J. Cioslowski, B. B. Stefanov, G. Liu, A. Liashenko, P. Piskorz, I. Komaromi, R. L. Martin, D. J. Fox, T. Keith, M. A. Al-Laham,

- C. Y. Peng, A. Nanayakkara, M. Challacombe, P. M. W. Gill, B. Johnson, W. Chen, M. W. Wong, C. Gonzalez, J. A. Pople, *Gaussian 03 (Revision C.02)*, Gaussian, Inc., Wallingford CT, **2004**.
- 26 a) J. M. Seminario, A. G. Zacarias, J. M. Tour, *J. Am. Chem. Soc.* **1998**, *120*, 3970. b) R. Thomas, S. Lakshmi, S. K. Pati, G. U. Kulkarni, *J. Phys. Chem. B* **2006**, *110*, 24674. c) H. Liu, P. Li, J. Zhao, X. Yin, H. Zhang, *J. Chem. Phys.* **2008**, *129*, 224704. d) P. V. James, P. K. Sudeep, C. K. Suresh, K. G. Thomas, *J. Phys. Chem. A* **2006**, *110*, 4329.
- 27 U. H. F. Bunz, *Chem. Rev.* **2000**, *100*, 1605.
- 28 S. W. Watt, C. Dai, A. J. Scott, J. M. Burke, R. L. Thomas, J. C. Collings, C. Viney, W. Clegg, T. B. Marder, *Angew. Chem., Int. Ed.* **2004**, *43*, 3061.
- 29 P. Samorí, V. Francke, V. Enkelmann, K. Müllen, J. P. Rabe, *Chem. Mater.* **2003**, *15*, 1032.
- 30 J. Kim, T. M. Swager, *Nature* **2001**, *411*, 1030.
- 31 G. L. Closs, M. D. Johnson, J. R. Miller, P. Piotrowiak, *J. Am. Chem. Soc.* **1989**, *111*, 3751.
- 32 T. Namikawa, M. Kuratsu, M. Kozaki, T. Matsushita, A. Ichimura, K. Okada, A. Yoshimura, N. Ikeda, K. Nozaki, *J. Photochem. Photobiol., A* **2008**, *194*, 254.
- 33 I. Gitsov, J. M. J. Fréchet, *Macromolecules* **1993**, *26*, 6536.
- 34 a) W.-S. Li, D.-L. Jiang, T. Aida, *Angew. Chem., Int. Ed.* **2004**, *43*, 2943. b) Y. Tomoyose, D.-L. Jiang, R.-H. Jin, T. Aida, T. Yamashita, K. Horie, E. Yashima, Y. Okamoto, *Macromolecules* **1996**, *29*, 5236.
- 35 a) A. Osuka, M. Ikeda, H. Shiratori, Y. Nishimura, I. Yamazaki, *J. Chem. Soc., Perkin Trans. 2* **1999**, 1019. b) S. A. Vail, P. J. Krawczuk, D. M. Guldi, A. Palkar, L. Echegoyen, J. P. C. Tomé, M. A. Fazio, D. I. Schuster, *Chem.—Eur. J.* **2005**, *11*, 3375.
- 36 Y. Araki, O. Ito, *J. Photochem. Photobiol., C* **2008**, *9*, 93.